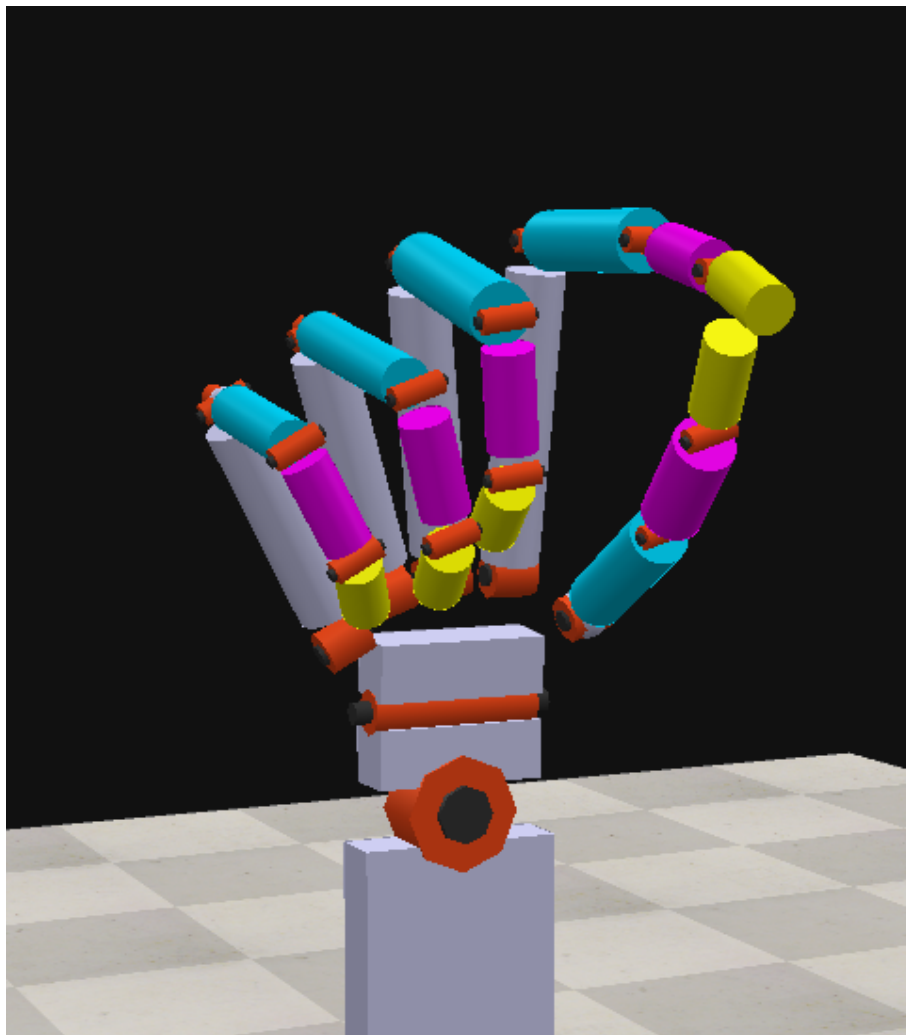


# Surface-EMG Processing & Classification for Muscle Interfaces

Thomas Alexgaard Jensen (tjens18@student.sdu.dk)  
University of Southern Denmark

Supervisors:  
Poramate Manoonpong (poma@mmmi.sdu.dk)  
Xiaofeng Xiong (xizi@mmmi.sdu.dk)

1. June 2023



## Abstract

The human upper-limbs are some of the most important appendages of the human body. The upper limbs of a human allows for interaction and manipulation of the environment, and acts as a crucial part of a functioning human body. The loss of an upper limb, either congenital or traumatic severely reduces a person's ability to interact with- and perform simple day-to-day tasks in the environment required for basic human living. This is a major problem for the amputee, and can only be partially solved by rehabilitation using a crude prosthetic device, designed to provide a interface between a mechanical or robotic appendage, and the remaining appendage section of the amputee. These prosthetic devices often only allow for a small degree of control through a limited interface at the attachment point of the prosthetic. This often causes the amputee to neglect the rehabilitation and usage of the prosthetic, by choosing to reserve it for limited use, or reject it all together. Amputees not choosing to make use of a prosthetic device, often cause overuse of their remaining limbs. This thesis aims to decrease the gap between existing prosthetic devices and their real-life counterparts, with the purpose of increasing dynamic control and reduce the amount of manual manipulation from the amputee. Doing so, hopefully decreases the amount of amputees choosing to reject their prosthetic device. Different control methods for prosthetic devices is researched, with a focus on processing and interpreting surface-electromyography data recorded from the upper appendage and the upper body. The different control methods compared are variations of different methods in Machine Learning and Artificial Intelligence, with the purpose of creating a model suitable for classification or regression in order to convert muscle recordings into a controllable output for a prosthetic device. This thesis proposes the use of feature-based Linear Discriminant Analysis for intent classification, and the usage of a 4-layer Recurrent Neural Network to predict the joint movements of the hand. A method of creating a state of the art training dataset is explored, this dataset is proposed to be created with the Motive motion capture system, in cooperation with the Delsys Trigno muscle recording system, and a custom made motion capture recording glove for the joint movements of the hand. Lastly, an anatomically correct simulated prosthetic hand is proposed, the simulation is designed to visualize and test control methods of a prosthetic device.

## Acknowledgements

This thesis is written by Thomas Alexgaard Jensen (tjens18@student.sdu.dk), a master's degree robotics engineering student at the University of Southern Denmark (SDU), in the period July 2022 to May 2023. This thesis is written under the supervision of Poramate Manoonpong (poma@mmmi.sdu.dk) & Xiaofeng Xiong (xizi@mmmi.sdu.dk) as part of SDU Biorobotics. I would like to thank my supervisors Poramate Manoonpong & Xiaofeng Xiong for granting access to Biorobotics Lab, and the usage of the Motive Motion Capture system in combination with the Delsys Trigno muscle recording system. I would like to thank Poramate Manoonpong & Xiaofeng Xiong for helping me realize my passion project of researching methods of developing prosthetic devices. Lastly, I would like to thank Poramate Manoonpong & Xiaofeng Xiong for providing meetings, help and relevant research papers during the development of this thesis.

I would like to thank my fellow student Kristian Varming for providing help with the usage of the Motive Motion Capture system. I would like to thank my fellow students Erik Lindby, Mikkel Werge Olsen & Claus Huynh for continuous conversations about development goals and directions that greatly helped the direction and development of this thesis. I would like to thank my friend Frederik Tørnstrøm, for providing motivational support and development conversations during the development of the thesis. Lastly, i would like to thank my family for providing motivational support when it was needed the most.

## Glossary

**abduction/adduction** Movement away/towards the midline of the hand. 17, 23

**BCI** brain computer interface. 14

**CNN** convolutional neural network. 12

**congenital** A disease or physical abnormality present from birth. 7

**Distal phalanx** The last bone located at the tip of the finger. 16

**ECG** Electrocardiographic. 12

**EMG** electromyography. 11

**ESN** echo state network. 14

**flexion/extension** The bending movement of the finger. 16, 17, 19

**goniometer** A measurement device designed to measure angles based on rotation of a center joint. 13

**HMI** human-machine-interface. 11, 14

**iEMG** intramuscular-electromyography. 11

**Interphalangeal joint** joints between the finger bones. 20, 43

**iRMS** integral root mean square. 13

**LDA** quadratic discriminant analysis. 13–15, 28, 43

**MAV** mean absolute value. 13

**Middle phalanx** Middle bone of the finger. 16

**ML** machine learning. 12, 14, 26

**MLP** recurrent multilayer perceptron. 13

**NARX** autoregressive exogeneous network. 13

**PCA** principal component analysis. 12, 14

**phalanges** All the bones of the fingers. 16

**Proximal phalanx** The first bone located at the base of the finger. 16

**QDA** quadratic discriminant analysis. 27, 28, 43

**RMS** root mean square. 13

**RNN** recurrent neural network. 13

**sEMG** surface-electromyography. 8, 11

**SHAP** Southhampton Hand Assessment Procedures. 12, 20

**SNR** signal-to-noise-ratio. 11

**specular reflection** Surface reflection that mirrors the direct light reflections in the scene. 21

**SVM** support vector machine. 14, 15, 26, 28, 29, 43

**traumatic** A disease or physical abnormality due to trauma. 7

**ZC** zero crossing. 13, 39

# Contents

<b>1</b>	<b>Introduction</b>	<b>7</b>
<b>2</b>	<b>Problem Specification</b>	<b>8</b>
2.1	Motivation . . . . .	9
2.2	Goals . . . . .	10
<b>3</b>	<b>Literature Review</b>	<b>11</b>
3.1	Introduction to Literature . . . . .	11
3.2	Noise in EMG signals . . . . .	11
3.3	sEMG Sensors for Prosthetic devices . . . . .	12
3.4	Adaptive Grasping Methods . . . . .	13
3.5	Grasping Intention from the Upper-arm . . . . .	13
3.6	Alternatives to sEMG-based Prosthetic Devices . . . . .	14
3.7	Summary of Literature . . . . .	14
<b>4</b>	<b>Methodology</b>	<b>16</b>
4.1	Research Approach . . . . .	16
4.2	Anatomy of the Lower-Arm . . . . .	16
4.2.1	sEMG Sensor Locations on the Body . . . . .	17
4.3	Design of a Motion Capture Glove . . . . .	19
4.4	Dataset Creation . . . . .	20
4.4.1	Existing Datasets . . . . .	21
4.4.2	Problems with Motive Tacking Software & Capture Glove . . . . .	21
4.5	Cleaning of Recorded Dataset . . . . .	22
4.6	Design of a Simulated Prosthetic Hand . . . . .	22
4.6.1	Simulated Hand Articulation design . . . . .	23
<b>5</b>	<b>Datasets</b>	<b>24</b>
5.1	Created Dataset . . . . .	24
5.2	Implementation . . . . .	24
5.3	Tests & Results . . . . .	25
5.4	Evaluation . . . . .	26
5.5	Cleaning of Motive Capture Data . . . . .	26
5.6	Dataset used for Training . . . . .	26
<b>6</b>	<b>Machine-Learning Intent Classification</b>	<b>26</b>
6.1	Implementation . . . . .	26
6.2	Tests & Results . . . . .	27
6.3	Evaluation . . . . .	29
<b>7</b>	<b>Neural Network Movement Regression</b>	<b>31</b>
7.1	Windowed Convolutional Neural Network . . . . .	31
7.1.1	Implementation . . . . .	31
7.1.2	Tests & Results . . . . .	32
7.1.3	Evaluation . . . . .	33

7.2	Recurrent Neural Network Regression . . . . .	33
7.2.1	Tests & Results . . . . .	34
7.3	Evaluation of Regression Methods . . . . .	35
<b>8</b>	<b>Simulated Prosthetic Hand</b>	<b>36</b>
8.1	Useability of the Simulated Prosthetic Hand . . . . .	36
8.2	Method . . . . .	36
8.3	Test & Results . . . . .	36
8.4	Evaluation . . . . .	36
8.5	Posing based on Network Output . . . . .	38
<b>9</b>	<b>Discussion</b>	<b>39</b>
<b>10</b>	<b>Conclusion</b>	<b>41</b>
10.1	Future Work . . . . .	42
<b>11</b>	<b>Bibliography</b>	<b>43</b>
<b>A</b>	<b>Prosthetic Hand Simulation in CoppeliaSim</b>	<b>47</b>
<b>B</b>	<b>Hand Simulation Poses</b>	<b>47</b>
<b>C</b>	<b>ROS2 Controller for the Prosthetic Hand</b>	<b>47</b>
<b>D</b>	<b>Modification &amp; Replaying Scripts for Motive CSV Files</b>	<b>47</b>
<b>E</b>	<b>Motion-Capture &amp; sEMG Dataset</b>	<b>47</b>
<b>F</b>	<b>Motive Marker labeling &amp; Uncleaned marker set</b>	<b>47</b>
<b>G</b>	<b>Pre-Processing Filter Graphs</b>	<b>47</b>
<b>H</b>	<b>Network Creation/Training/Testing Code</b>	<b>47</b>

# 1 Introduction

The human hand is one of the most important factors of the human identity. The hand allows a person to perform complex muscular control combinations to interact with the surrounding world, express complex emotions during speech, and aid in defining a person's individuality and personality [1]. The hands are controlled by a complex combination of precise muscles designed to perform gentle, precise control of the fingers. This allows a person to grasp objects in many different ways, perform complex tasks such as writing, playing musical instruments, or even constructing a house. The hand also acts like a sensory device allowing us to perform precise observations through feeling and touch. This allows a person to understand the environment without seeing it, the hand is able to sensor temperature, create complex understanding of geometries and texture through touch and manipulation. Missing limbs, either congenital or traumatic amputation severely reduces a person's ability to interact with and understand the world, express themselves and perform simple day-to-day tasks. In order to alleviate some of the drawbacks of missing a limb, amputees are often able to acquire a prosthetic replacement of their lost limb. The development of prosthetic devices dates back thousands of years [2]. Early prosthetic devices would often be fashioned from metal or wooden components, with passive joints enabling crude movements of the device. There has been a large historical development in the area of controllable prosthetic devices, actuated mechanisms controlled by cable-transmission of tension through upper body would allow simple control of an end gripper. More modern prosthetic devices makes use of electronic actuation to simulate the movements of real limbs. The modern prosthetic devices tries to imitate the movements of the lost limb, through muscle-activated interfaces used to imitate movements of the real limb. The upper-body limbs is much more complicated in design and function than the lower-body limbs. Lower-body prosthetic devices are often mechanical, designed to provide a stable platform for walking [3]. Imitated functionality of the upper-body limb is much more difficult to design, and requires robotic parts that can actively move and conform based on the user's intention and the objects of interaction in the environment. In the case of prosthetic hands, it is crucial that the prosthetic allows the user to perform simple day-to-day tasks.

Statistics show that in 2017,  $\sim 57.7$ million people were living with amputation due to a traumatic occurrence [4]. This indicates that prosthesis research and development would be highly beneficial worldwide. Research in prosthetic devices and their integration with the human body is a crucial part of increasing amputee social functionality and increase their day-to-day functionality. The development of this thesis is dedicated to the constantly growing need for prosthesis research and development, with the purpose of increasing the usability and control of robotic prosthetic devices. The focus area of this thesis is centered around robotic upper-limb prosthetic devices due to its complicated interface requirements and its higher need for dynamic control.



## 2 Problem Specification

There is a large need for new technology that improves the effectiveness and ergonomics of human hand prosthetic devices. Current state-of-the-art prosthetic products on the market exhibits a severe reduction of controllable degrees of Freedom compared to their biological counterparts. Some prosthetic hand products are simple in design, often using a small set of motors to control multiple joints at the same time, furthermore, these products often rely on simple, grasp control based on 2 or more surface-electromyography (sEMG) interfaces. These sEMG interfaces are used to classify “open” and “close” signals generated by the muscles in the residual limb of the amputee. The user of the prosthetic hand is manually required to change control-scheme between different grip types, creating very crude control dynamics that is fundamentally different from biological hand control. An example of a commercial prosthetic with this crude control design is the “Ottobock Bebionic Hand EQD” [5]. The Ottobock hand is marketed as being a comfortable, intuitive & adaptable prosthetic hand giving you natural and precise control of a wide range of grip types. This is however far from the truth when reading the usage manual, that states that changing between grip types can be done by pressing a button on the top of the device for a second. Furthermore, in order to move the thumb rotation joint, the user is asked to manually rack the thumb to the desired position. None of these usage patterns provide meaningful and dynamic adaptability of the device, and is in no way intuitive compared to a real hand. The Ottobock Bebionic Hand EQD is priced at \$30,000 to \$40,000 [6]. The control pattern used in the Ottobock prosthetic hand follows the scheme shown in figure 1.

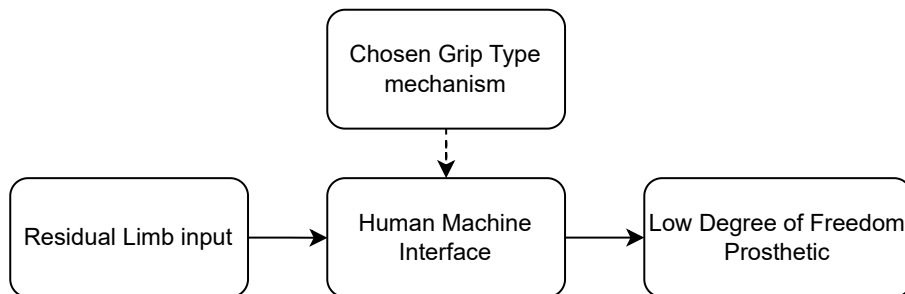


Figure 1: Example of a commercial prosthetic hand’s manual control scheme [5].

Crude control of upper-limb prosthetic devices is a great pitfall in the field of research and development of prosthesis, this has a large impact on rehabilitation of amputees. The World Health Organization (WHO) defines rehabilitation as “a set of interventions designed to optimize functioning and reduce disability in individuals with health conditions in interaction with their environment” [7]. Proper amputee rehabilitation and insight in the function of the prostheses is crucial to the independence of the amputee, but unsatisfactory function of prosthetic device lead to amputees, that exhibit a great deal of stress during the rehabilitation process. Dissatisfaction and stress can cause the patient to repel the rehabilitation process and the prosthetic all-together [8]. The repelling of the prosthesis increase in the cases of the most severe cases of amputation, where the largest amount of control muscles are

lost. These amputations are often located further up the limbs, where the resulting loss is the largest. The type of prosthetic the amputee is able to receive is highly dependent on the severity of the loss of limb, furthermore, the amount of muscles leftover from amputation also dictates the type of prosthetic interface the patient is able to interface with. Patients of hand amputation are able to receive prosthetic devices with much more control of individual movements due to the muscles controlling the fingers being intact. Lower-arm amputation patients has less control over their prosthetic due to the loss of the muscles in the lower-arm. The differences between amputation severity is a problem in prosthesis design because it is impossible to create a standardized prosthetic that suits most patient's needs.

## 2.1 Motivation

The main goal of this thesis is to provide a meaningful contribution to the world of prosthesis design and control. Modern state-of-the-art commercial prosthetic hands are in no way comparable to their real life counterparts. The ideal control scheme of a prosthetic device is the control-scheme used by a real human hand, this control scheme can be seen in figure 2.

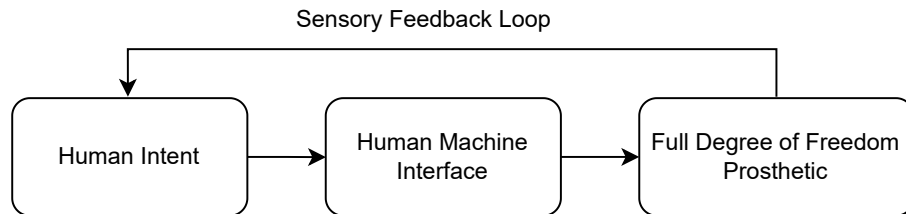


Figure 2: The Ideal design of a prosthetic hand, that mimics the control scheme of a real hand.

This thesis aims to contribute to the world of prosthesis control, and by doing so, research methods of bringing current state-of-the-art prosthetic devices closer to their real life counterparts. This gap exists in terms of control and dynamic modification of grip types, and will be focused on by researching effective methods of collecting sensory data from the upper appendage. By researching effective data collection methods, it is hoped that the contribution of the thesis would be shifting modern methods closer to an adaptive controller that is able to imitate the intent and movements of a real hand. Increasing the dynamic control of a prosthetic, by improving data collection and interpretation of muscle signals, will provide a more true-to-life experience to the prosthesis user, and hopefully reduce the amount of patients that disregard prosthetic devices, and increase overall amputee independence. Lastly, this thesis aims to design a simulated, anatomically correct prosthetic hand with the purpose of testing the developed methods.

## 2.2 Goals

In order to define the research and development of this thesis, a set of development goals has been made:

1. Create a software-based, biology-inspired, anatomically realistic simulation of a humanoid lower-arm and hand that is able to imitate the movements of the human hand.
2. Create a dynamic software interface to control the software-based prosthetic hand using a widely-used robotics communication interface.
3. Research and design sEMG based pre-processing pipelines for a prosthetic device controller, with the purpose of eliminating noise and increasing meaningful aspects as input to a controller.
4. Research and design state-of-the-art prosthetic device controllers based on machine learning and artificial intelligence, with the focus of increasing overall control and dynamic adaptability of a simulated prosthetic hand.
5. Design a set of core day-to-day movement types of the hand, that can be reproduced by 1 or more people in order to create a dataset applicable to train the designed controller models.
6. Test and Validate the created controller models on the simulated prosthetic hand, in order to assess the applicability of the designed methods.

### 3 Literature Review

As the capability of sensor technology increases, the possibilities in biological signal processing, becomes more important in state-of-the-art prosthesis development and research. There is a larger need for understanding and translating human-created sensor data into usable inputs for prosthesis and other human-machine-interface (HMI) devices. A lot of research has been done in this area, this research elaborates on different Machine learning or AI-based methods of understanding muscle-based sensor data. The pipeline for converting sEMG sensor recordings to usable input data often starts with a pre-processing step, where noise is removed from the recorded data, and cleaned of potential misreadings. The pre-processing step is followed by a processing step, this step encompasses the use of a Machine-learning algorithm or a Neural Network, designed to either Classify a grip type, or Regress the angle of the joints. After Classification or Regression a post-processing step can be added where the actual kinematic data is created, and used as input to the prosthetic controller. Popular methods of processing sEMG signals will be researched, and elaborated upon, with the aim of identifying robust, effective and implementable methodologies.

#### 3.1 Introduction to Literature

TODO: Something more general about control needs to be added so it isnt all about noise!

HMI's, are control systems that enables humans to interact and control a mechanical, software-based or robotic system. As explained in the paper [9], researchers and prosthesis developers have been developing robotic prosthetic devices for many years. The paper proposes that electromyography (EMG) signal based control research are a ongoing topic in rehabilitation and prosthesis research. Generally, EMG-based methods are split into two groups, namely sEMG & intramuscular-electromyography (iEMG). Where sEMG recording is the practice of non-invasive recording muscle activity from the surface of the skin on top of the muscle and iEMG uses invasive embedded electrodes to record activity from the inside of the muscle. Non invasive sEMG sensors provide much less discomfort and propose no risk of infection to the amputee, but the recorded data has a larger signal-to-noise-ratio (SNR). The muscle fiber membrane has a resting potential of  $-90$  to  $-90mV$  when resting. The paper also explains that the amplitude of sEMG signals have a voltage range from  $0$  to  $10mV$ , and a frequency range from  $10$  to  $500Hz$  [9].

#### 3.2 Noise in EMG signals

According to the paper [9], different noise types that contaminates EMG signals, these noises are defined as electrical signals that are not part of the desired EMG signal. The different noise types that combined contributes to most of the SNR in EMG signals are

- Inherent Noise in Electronics Equipment,

- Ambient Noise,
- Motion Artifacts,
- Inherent Signal Instability,
- Electrocardiographic (ECG) Artifacts,
- & Cross Talking.

**Noise in Electronics Equipment** exists in all electronic devices, this noise has been proved to be reduced by using electrodes made of silver. **Motion Artifacts** affects EMG signals when the skin and electrodes move in relation to the movement of the underlying muscle. This can cause artifacts due to inconsistent displacement. **Inherent Signal Instability**, The amplitude of EMG signals are quasi-random. Frequency components less than 20 Hz are unstable and affected by firing rate of the motor units. This range is considered unwanted noise. Muscles change based on their active motor units, therefore the EMG signal changes too. **ECG Artifacts** is the electrical activity of the human heart is a huge interference component of EMG signals recorded from the Shoulder Girdle (Shoulder muscle groups). It is very hard to remove ECG artifacts from EMG signals, due to their relative characteristics in the frequency spectrum! **Cross Talk** is undesired EMG signals from muscle groups not commonly monitored. It can be seen as a form of EMG signal leak from muscles not actively being recorded from.

### 3.3 sEMG Sensors for Prosthetic devices

The usage of sEMG sensors propose a lot of obstacles because of noise, but that does not stop sEMG sensors from being part of the state-of-the-art research in prosthetic devices. In the paper [10] proposes that the usage of sEMG sensors are of great importance in upper-limb classification for prosthetic devices. The paper uses sEMG sensors to classify reaching-to-grasping tasks using a convolutional neural network (CNN) after pre-processing the signal with principal component analysis (PCA) to reduce noise. The processing combination method of PCA-CNN is proposed as showing higher accuracy than machine learning (ML) methods. The paper proposes that the sEMG sensors are placed on the upper-body in combination with the upper-arm for grasping intention classification, specifically, the muscles *Pectoralis*, *Trapezius*, *Latissimus Dorsi* & the *Biceps* & *Triceps*, these are considered in section 4.2.1 as potential target muscles for recording. In [10], the *Southampton Hand Assessment Procedures (SHAP)* [11] was used to create a dataset. SHAP is designed for the assessment of musculoskeletal health and neurological conditions, and can be used to test the control and effectiveness of prosthetic devices.

Another paper that proposes the usage of sEMG sensors for prosthetic control is [12]. The paper proposes the usage of different sEMG devices, two of those are the wearable product “Myo Armband”, [13] a discontinued sEMG product consisting of 8 sensors that can be placed below the elbow joint, and the “Delsys Trigno” [14], a set of individual sEMG sensors that can be worn and record most muscle groups. [12] proposes the pre-processing of the sEMG data using a Notch filter of 50Hz.

Furthermore, the target angles obtained as ground truth targets were reduced in dimensions through PCA, thus having the 6 dominant PC's be the targets. Then, using an "Inverse PCA algorithm", they compute the final control output for the prosthetic. In order to process the sEMG data, [12] proposes the use of a time window of  $200ms$ , with feature extraction for root mean square (RMS) & zero crossing (ZC). The extracted features were used as input to a nonlinear autoregressive exogenous network (NARX), that consists of recurrent multilayer perceptron (MLP) layers combined with a recurrent neural network (RNN).

### 3.4 Adaptive Grasping Methods

Most state-of-the-art methodologies consist of using sEMG data to predict grasp type classification or joint angle regression. The paper [15] proposes that this method becomes a burden for the HMI user, as the severity of the amputation increases and the loss of muscle recording areas become greater. The paper takes inspiration from evolutionary robotics, and proposes the use of evolutionary computation to predict stable grasping methods based on touch sensor input. This is done by having a mapping between the touch sensor input of the fingers and the motor-control of the joints. A simulation is used to train a RNN network, this RNN takes sEMG sensor data, Touch sensor data, distance to the object & object height into account. It is possible to compute distance and height parameters of the object because grasping and training is done entirely in simulation, using a simulated target object, but that the method used would be realizable for prosthetic devices. The paper concludes that alongside sEMG sensors, touch sensors could be used to appropriate joint motion could be predicted using contact states between hand and object.

The paper [16] proposes a passive solution to adaptive grasping. Their method uses an under actuated, compliant linkage mechanism, where the joint rotation of the finger joints can be driven by a single motor. This allows the fingers to not rely on touch sensors, as the method in [15] does. The paper proposes the use of a sliding window with a size of  $250ms$ . The window is then processed using feature extraction of integral root mean square (iRMS), RMS, mean absolute value (MAV) & ZC with a threshold to eliminate low signal fluctuation from noise. The extracted features are used for linear discriminant analysis (LDA) to classify grasping intent. The paper proposes that LDA showed the highest accuracy out of different Machine Learning methods.

### 3.5 Grasping Intention from the Upper-arm

Another way of reducing the recording of lower-arm muscles when designing prosthetic hands would be to predict the intent of the user's actions based on upper-arm grasp prediction. The focus of the paper [17] on recording and classification of upper-arm. The paper proposes a learning approach that decodes grasping intention during the reaching motion for upper-limb prosthesis. For pre-processing, a  $30-350Hz$  band-pass filter is used on 12 muscles, 7 located in the upper-arm and 5 located in the lower-arm. These muscles are passed through a Butterworth filter with cut-off at  $20Hz$ . Furthermore, the elbow joint angle was measured using a go-

niometer. The paper proposes that a sliding window of  $150ms$  should be used, and they use no dimension reduction method such as PCA. The paper tests 2 different machine-learning methods, QDA and support vector machine (SVM), that utilize feature extraction of the average activation, waveform length and the number of slope changes for each window. Additionally, the paper tests a recurrent network called a echo state network (ESN) without windowing and feature extraction.

### 3.6 Alternatives to sEMG-based Prosthetic Devices

Research of control interfaces for prosthetic devices expand into a multitude of areas. The paper [18] proposes the use of a brain computer interface (BCI) as an alternative to HMI. BCI is a type of technology that uses brain activity and the brain's neural information to control machine interfaces such as computers, assistive technology & prosthetic devices. BCI's have great benefit in areas where access to muscle tissue information such as sEMG is impossible due to loss of the muscles in the target recording area, or due to a patient being paralyzed and it becomes impossible for the patient to activate the targeted muscle groups. One dominant method of achieving a BCI interface is electroencephalography (EEG). The purpose of [18] is to detect individual finger control using EEG sensors. EEG functions similarly to EMG but with the focus on recording brain activity instead of muscle activity. EEG is a non-invasive, portable and low-cost sensor type, that provides a high temporal resolution in comparison to other methods that detects brain activity, according to the paper [19]. The paper explains the great need for assisted rehabilitation and prosthetic devices, and that the need will increase in the future. Brain Computer Interfaces using EEG sensors needs to be further researched to increase overall performance of the system. The paper proposes that the most used method of controlling a prosthesis or a rehabilitation device using EEG is to pre-process and filter the recorded data before segmenting it using a sliding window. Using the windows, feature extraction in both time & frequency domains are used as input to a feature reduction algorithm. These features are then subject to a classification network in order to transform the EEG data into motor control for the BCI. It can be noted that the EEG sensor contains artifacts from other parts of the brain, such as eye movement, cardiac activity or contraction of the scalp muscles. Overall performance of using EEG for prosthetic device control is low compared to more conventional methods such as EMG [19]. Furthermore, the setup for EEG recording is more complicated than EMG.

### 3.7 Summary of Literature

The state-of-the-art literature spans different methods of creating human machine interfaces. The main areas of creating interfaces are Muscle-/neuron-based recording and brain-based recording. Due to the large amount of cross-talk noise from brain-based sensors, it is apparent that to increase overall dynamic control, and robustness of a prosthetic device, the device is required to use EMG based sensor for its controller. By reviewing the state-of-the-art literature in sEMG-based prosthetic hands, it is apparent that if a ML & neural network method, are to be used,

we need to use a sliding window technique with a size of  $150ms$  to  $250ms$ . It can be noticed that all methods use a pre-processing filter step on the raw EMG data, but that the choice of filter varies greatly. Among the most used filters are Butterworth low-pass & band-pass filters with different frequency responses. 3 different methods of classification/regression of sEMG data are used: Machine Learning, Window-Based Neural Networks, Recurrent Neural Networks. The most common ML methods used in literature is QDA, SVM & PCA-CNN. As an alternative to ML, most literature proposes the use of window based Neural Networks & recurrent neural networks.



## 4 Methodology

### 4.1 Research Approach

In order to design a simulated prosthetic device that facilitates the requirements stated in section 2.2, effective software solutions needs to be chosen.

A simulation software needs to be chosen in order to create a dynamic and controllable prosthetic hand simulation. The software needs to be controllable from an external source, in this case ROS2 [20], and because of this, software like Gazebo [21] or CoppeliaSim [22] is ideal. Both simulation software solutions allow for the creation of advanced dynamic-body simulations. CoppeliaSim [22] was chosen due to its intuitive development workflow.

In order to record the joint movements of the hand, while simultaneously record the sEMG activity of the body, products that support hardware synchronization needs to be used. Products designed to capture sEMG data are widely spread. As mentioned in the paper [12], the myo armband [13] or the Delsys Trigno package [23] could be used. The Delsys Trigno [23] facilitates a hardware synchronization recording mode out of the box, while the myo armband [13] does not. Because of availability, and synchronization capabilities it is ideal to use the Delsys Trigno as the sEMG recording device.

Lastly, a product designed to capture the joint movements of the hand needs to be chosen. A simple solution to hand tracking would be to use a software like MediaPipe [24], a python based landmark tracker that can track the joint angles of the hand using Machine Learning from a video feed. An alternative is mentioned in the paper [12], where a glove containing flex sensors could be used. This approach would provide reliable joint angle data without relying on a camera setup. Lastly, a capture glove could be fitted with 3D markers, detectable from a high-accuracy and high frame-rate system such as the Motive motion capture setup [25] created by OptiTrack. It was chosen to use the Motive setup due to availability and the additional benefit of having a hardware synchronization feature, that can be combined with the Delsys Trigno [23] setup.

### 4.2 Anatomy of the Lower-Arm

The hand is an anatomically-complex appendage designed to facilitate a large amount of control and adaptability in different usage scenarios. The hand consists of 27 bones, 14 of these are called the phalanges, and make up the 4 fingers and the thumb. These bones, alongside a complex network of  $\sim 30$  muscles are able to perform 24 degree of freedom (DoF) of rotational motion along the joints of the bones [26]. The individual finger consists of 3 bones called phalanges, arranged linearly from the palm of the hand, and can be seen in Figure 3. These bones are respectively called the Proximal phalanx, Middle phalanx & Distal phalanx. The different joints located in the hand have unique rotation properties. The joints between the proximal and distal phalanges have 1 DoF of independent movement and are able to do flexion/extension movement. The base of the proximal phalanx has 2 DoF and are

able to do flexion/extension & abduction/adduction movement. Additionally, the joint between the middle and distal phalanx is passively moved relative to the proximal and distal phalanx, or in relation to joint constraints from gripped objects. The wrist consists of 8 small bones and together creates 2 DoF with flexion/extension & abduction/adduction movement.

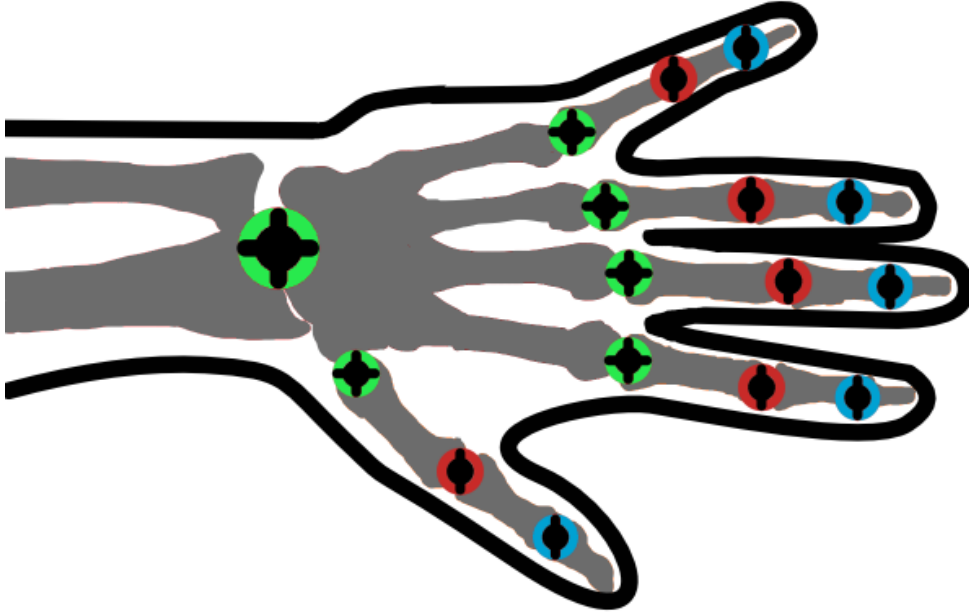


Figure 3: A rendering of the anatomical joint structure of the hand. 2 DoF joints are colored in green, 1 DoF joints are colored in red, and passive 1 DoF joints are colored in blue.

#### 4.2.1 sEMG Sensor Locations on the Body

To create a dataset that correlated muscle activity to the movements of the hand, it is important to choose a set of active muscles to record.  $\sim 30$  muscles are used in total to control the hand, but it would not be possible to record all of them simultaneously. 6 sEMG sensors were available in the Delsys Trigno [14] system, and these needed to be placed optimally in order to increase recording of the most important muscles. Target areas on the lower-arm for sEMG sensors are proposed by the paper [27]. Additionally, target areas of the upper-arm & upper-body were chosen based on the suggestions from the paper [17]. The chosen muscles to record with sEMG sensors can be seen in Table 1.

Muscle	Main Functionality
(A) <i>Flexor Digitorum Superficialis</i>	Flexion of the 4 fingers
(B) <i>Extensor Digitorum</i>	Extension of the fingers
(C) <i>Extensor Carpi Radialis Longus</i>	Wrist extension & hand abduction
(D) <i>Triceps Brachii (long head)</i>	Extension of the arm
(E) <i>Biceps Brachii</i>	Flexion of the arm
(F) <i>Pectoralis Major + Frontal Deltoid</i>	Movement of the Arm

Table 1: The muscles targeted with the 6 available sEMG sensors, as recommended by the papers [27] & [17]. The targeted muscles contributes to a lot of the movements of hand & lower-arm, and are ideal for the dataset.

The target muscles were chosen as they contribute to a lot of the overall movements of the hand & lower-arm. The muscles in Table 1 are numbered, and the locations of the individual sensor with the corresponding muscle can be seen in Figure 4.

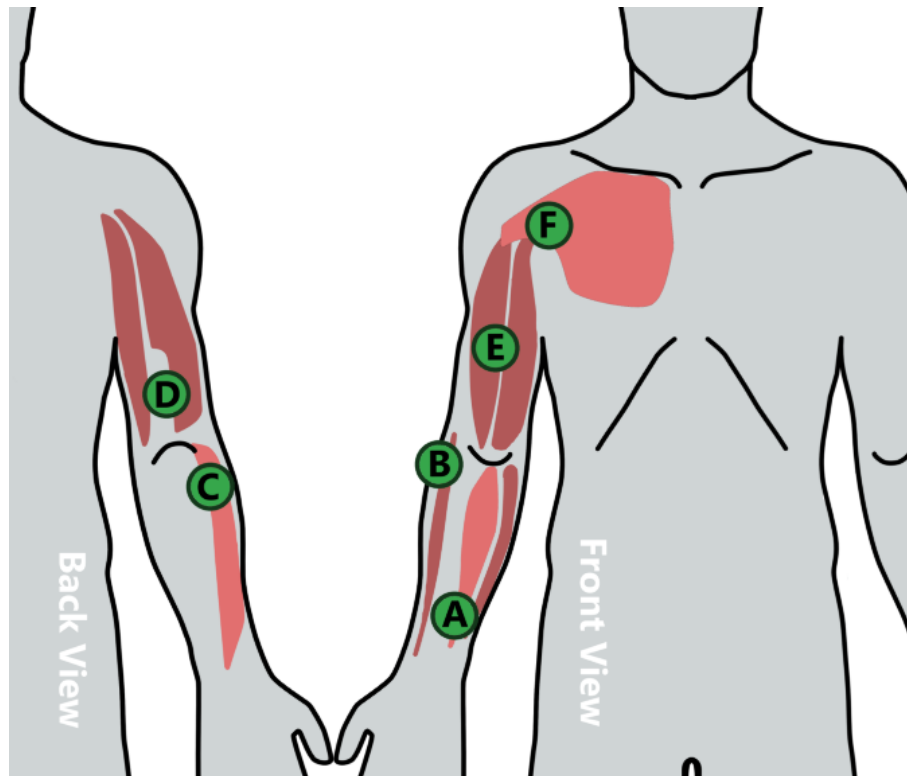


Figure 4: Muscle diagram, containing the target sEMG locations. The numbering corresponds to the muscle names in Table 1. The left image shows the muscles on the rear of the arm, while the right shows the muscles on the front of the arm.

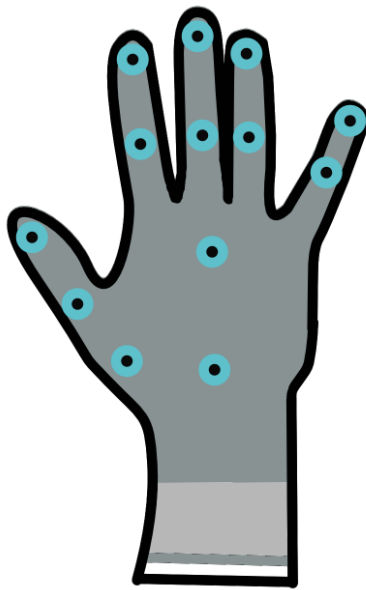
It was chosen to split the amount of sensors evenly along the lower-arm and the rest of the body in order to assess both direct control of the finger movement and intent based on upper-arm movements. Alternative muscles that would be interesting to test are the back muscles, namely *Trapezius* & *Latissimus Dorsi* as proposed in [10].

### 4.3 Design of a Motion Capture Glove

The motion capture system created by OptiTrack [28] is a set of 8 high-quality cameras mounted to cover a target capture area. The capture system detects fluorescent 3D markers in the given capture area, with the purpose of triangulating the markers and effectively calculate 3D poses for the markers in the scene down to an effective accuracy of  $\pm 0.2mm$ . In order to get precise recordings of the motion of the hand and fingers, fluorescent 3D markers were placed on a glove. The pattern of the marker positions were chosen in order to calculate the angles of the individual finger bones. The markers are used in sets of 3, this allows for the calculation of the triangle angles in 3D space. The positions of the 3D markers on the recorder glove can be seen in Figure 5a & 5b. An example of flexion/extension movement of the capture glove can be seen in Figure 6a & 6b.

Due to the placements of the 3D markers, the joint angles are calculated by defining two vectors from the target 3D marker and using Equation (1):

$$\alpha = \cos^{-1} \left( \frac{\vec{a} \cdot \vec{b}}{|\vec{a}| \cdot |\vec{b}|} \right) \quad (1)$$



(a) 3D marker location design.



(b) Created motion capture glove.

Figure 5: (a) Design and ideal 3D marker placements on the glove in order to calculate all the joint angles of the hand. (b) The created 3D marker glove with the chosen 3D marker locations. See section 4.4.2 for detail.

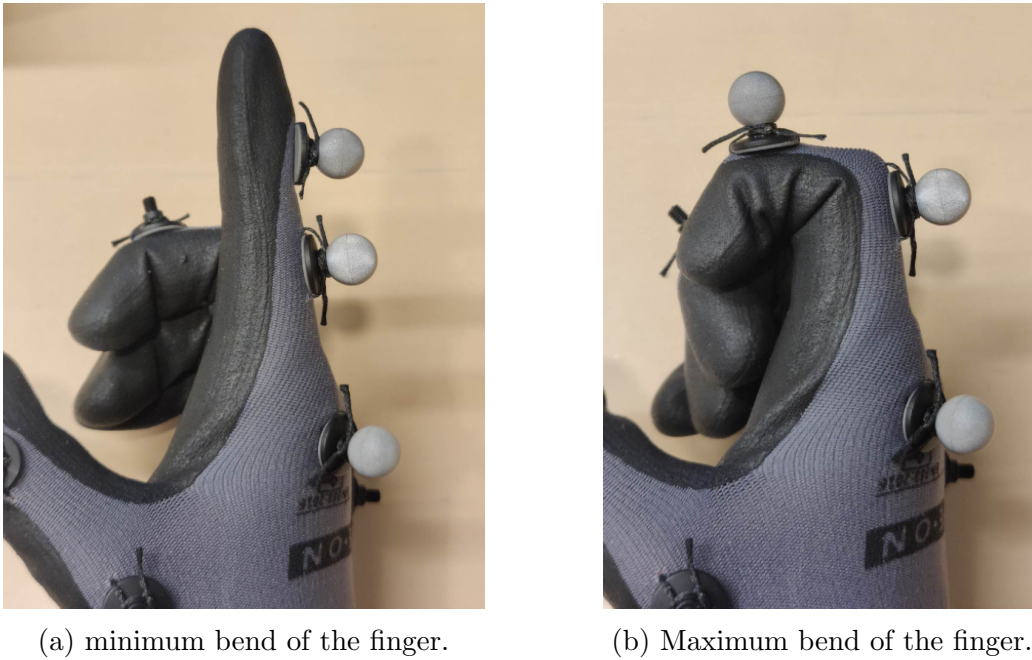


Figure 6: Visualization of the joint angle retrieval process. (a) the minimum bend of the Interphalangeal joint, (b) the maximum bend. The joint angle can be calculated from the 3D markers by denoting vectors from the center marker to upper and lower markers, and using Equation (1).

#### 4.4 Dataset Creation

In order to create a controller for a prosthetic hand, a sophisticated dataset containing the measured relation between muscle activity and the finger placements is needed. For such a dataset to represent meaningful data, that can be used to train sophisticated controllers for prosthetic devices, it is important that the dataset is made up of the relevant day-to-day manipulation movements. The paper [10] proposes the SHAP [11] as its main method of dataset creation, an alternative would be the “Sollerman Hand Function Test” [29]. Both procedures are used in assessing the function and mobility of the human hand. By analyzing the most important gripping motions in both tests, it should be possible to denote a suitable set of grips that the dataset needs to contain. The sollerman grip types are ranked based on their usage percentage in activities of daily living. From this, the most used grip types according to sollerman are the *Pulp pinch*, *Lateral pinch*, *Five-Finger pinch* & *Diagonal Volar grip (Power grip)*, see [29] for further details. SHAP also proposes a set of grip types that are used in day-to-day tasks, these are *Spherical grip*, *Tripod pinch*, *Power grip* & *Lateral pinch*. In order to create a dataset mimics the movements of day-to-day tasks, the most important grips from [29] & [11] has been chosen. The grip types that needs to be part of the dataset and their usage descriptions can be seen in Table 2. A set of concise grip types has been chosen as an alternative to a larger set of general grips. This is done as a basis of creating a specialized dataset that would be easier to train and work with as a proof of concept.

Grip Type	Object Placement Description
Pulp pinch	Between thumb, index and middle finger
Lateral pinch	Between thumb & side of index finger
Five-Finger pinch	Between thumb, and all four fingers
Power grip	Between thumb, and all four fingers with contact to palm

Table 2: The most used hand grips in day-to-day tasks based on *Southampton Hand Assessment Procedure* [11] & *Sollerman Hand Function Test* [29].

#### 4.4.1 Existing Datasets

In addition to creating a dataset for this thesis, an existing state-of-the-art dataset will be used and compared with. The paper [27] proposes the use of their dataset [30]. The dataset contains a very large set of recordings, with 3 different labeled states, consisting of precise anatomical angles of the hand, with the associated muscle activity of the forearm. This makes the dataset ideal for both classification and regression based models. The dataset consists of 572 recordings from 22 subjects, in both reaching, gripping & releasing actions. Another dataset is explained in the paper [31], as an alternative of using finger joint angles as the ground truth data needed to train a network on sEMG data, the dataset uses a set of 16 gesture classes for a classification algorithm. The paper explains that the sEMG data in the dataset has been subject to a pre-processing step using a 10 to 500 $Hz$  Buttersworth bandpass filter, and in order to remove power-line noise a 60 $Hz$  notch filter was used. The dataset was created on 43 participants.

#### 4.4.2 Problems with Motive Tacking Software & Capture Glove

During testing and the creation of the dataset, several problems with the capture glove design and the capture setup became apparent. These problem severely reduced the amount of time available to create and process a large dataset for this thesis. The Motive Motion Capture software [28] had a lot of difficulty with finding, recording and optimizing the 3D markers placed on the capture glove.

The Motive software used to generate the 3D poses is designed to detect 3D markers in the scene. Once the markers are found in the individual cameras, they are subject to an optimization algorithm that effectively tries to determine if the markers seen in 1 camera is the same as the markers in the other cameras. The first problem that occurred was specular reflection in the scene caused by shiny surfaces redirecting light in the target area. This creates *phantom* markers that can be seen in only a small set of frames. Another problem with the capture setup is the optimization algorithm. During recording of the dataset, it became apparent that it would not be possible to record multiple fingers at the same time. 3D markers very close to each other seemed to be connecting, and only become a single marker in the tracking software. This problem specifically occurred when the markers at the finger tips of the glove came in contact with each other causing marker data to be lost. Furthermore, the Motive Capture software uses an auto-labeling system that is able to determine if the markers seen in one frame, are the same markers in the next

frame. This system proved to not be reliable, giving  $\sim 200$  labeled marker sequences, when only 7 markers existed in the scene. The amount of markers increased as 30 seconds of footage became create  $\sim 1000$  marker labels. The unreliable labeling of markers can be seen in appendix F.

## 4.5 Cleaning of Recorded Dataset

TODO: This section could be expanded and images could be included.

The large amount of problems observed using the Motive Motion Tracking software makes it impossible to use the tracking output as training data. The problems requires the user to manually combine labeled marker sections into larger labeled sections, in order to reduce changing labels on the tracked markers. It would be ideal if this functionality existed in the Motive software, but this was not the case. Because of a lack of functionality in Motive, software was created to replay the 3D markers in real-time, with their associated labels. Furthermore, software that was able to remove, merge and sub-sample markers was used to clean the labels. The software created to fix unreliable labeling of markers can be seen in appendix F.

## 4.6 Design of a Simulated Prosthetic Hand

In order to design a state-of-the-art simulated prosthetic hand based on the goals in section 2.2, a number of anatomical design choices needs to be considered. Designing the simulated prosthetic to as anatomically-correct as possible will hopefully have a number of positive effect on the resulting movement characteristics of the hand, and make it easier to imitate the movements of its real life counterpart. By having access to an advanced simulation, it would in turn be able to test and visualize more advanced movement controllers that can facilitate more DoF than current commercial prosthetic hands. By creating an anatomically correct prosthetic hand simulation, it is hoped that prosthesis users can have more advanced rehabilitation, and learn to have more natural control of their prosthetic devices. This would create a more natural usage experience, and decrease the percentage of users that reject the usage of their prosthetic all together. A set of requirements The simulated anatomically correct hand should be determined in order to create a state-of-the-art prosthesis simulation. The simulated prosthetic should:

1. Facilitate the same DoF as an anatomically correct hand.
2. Have proportions that closely resemble that of an anatomically correct hand.
3. Be simulated and be controllable in a commonly used robotics software to increase accessibility for researchers.

The resulting prosthetic hand simulation can be seen in appendix A.

#### 4.6.1 Simulated Hand Articulation design

In order to translate the biology and anatomy of a real hand explained in section 4.2 into an robotics simulation, the relative lengths of the wrist bones and phalanges were used as reference. The resulting hand model can be seen in Figure 7.

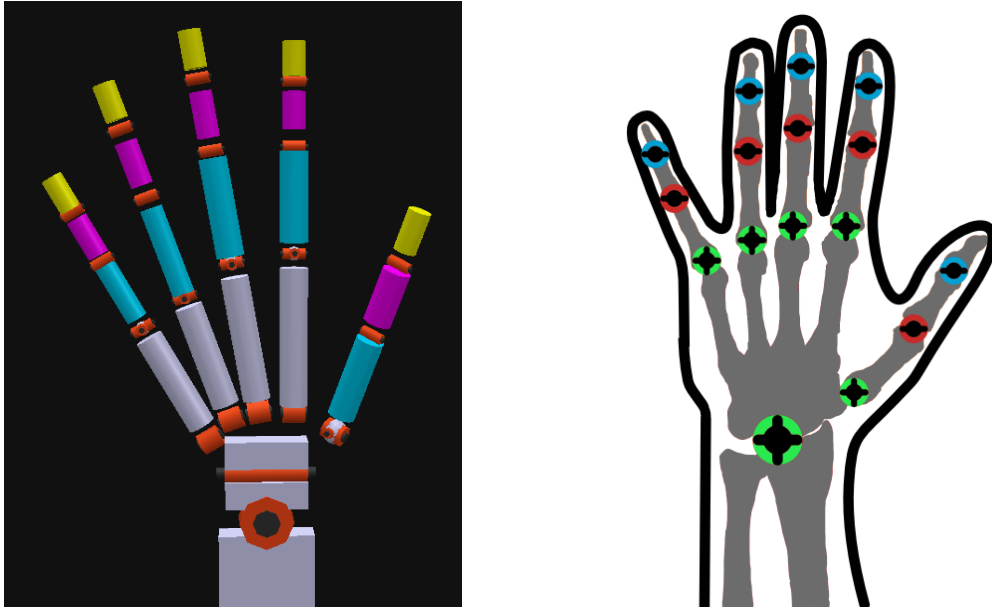


Figure 7: Created & anatomical reference design for the created simulated prosthetic hand.

The model is implemented in CoppeliaSim [22], and is based on cylinder shapes of anatomically accurate length and positions. The phalanges have been colored, with the distal phalanx being yellow, the middle phalanx being purple and the proximal phalanx being blue. As specified in section 4.2, some joints of the human hand facilitate 2 DoF of rotation. This is needed in order for the wrist and finger base joints to be able to do abduction/adduction. To simulate this, two 1 DoF revolute joints were placed in series, thus allowing 2 DoF of motion in a single joint.



## 5 Datasets

### 5.1 Created Dataset

The created capture glove for the Motive motion capture system and the sEMG sensors from the Delsys Trigno setup is placed on the target, with the sEMG sensors following the setup in 1. The setup can be seen in Figure 8. Objects of different sizes and weights is placed in front of the target for gripping. This is done so that the chosen gripping sequence and environment is highly dynamic, and ideal for creating regression models.



Figure 8: Capture glove and sEMG sensors placed on the recording target. The sEMG sensors are located based on the muscles from table 1.

As explained in section 4.4.2, creation of a custom dataset to train and test models on proved to be difficult. The dataset created using the Motive capture software in section 4.3 is not very large, and has no labeling for classification. Because of this, the dataset is not suitable for training in any of the methods.

### 5.2 Implementation

Based on the literature review in Section 3, it becomes apparent that there exists a standard pipeline for translating sEMG recordings into predicted motor control for a prosthetic. Raw sEMG data contains a lot of unwanted noise as explained in section 3.2. Some of the noise can be removed through signal processing using analog filters. Different filter types exist, and different filters are used to remove a specific frequency in the data. State-of-the-Art papers use a lot of different methods to reduce noise in sEMG data. The paper [32] proposes the use of a  $50Hz$  Notch filter, while papers [33] & [31] respectively choose a  $20Hz$  cutoff Butterworth filter & a  $10 - 500Hz$  Butterworth band-pass filter, lastly the paper proposes a  $60Hz$  notch filter in order to remove power-line noise. Due to many different filtering types used in state-of-the-art literature, it was determined that the use of a filter depends on the specific sEMG data and the purpose of what the paper tries to do. In order to determine what types of filters have a positive effect on the sEMG data recorded

using the Motive Capture system, different types of state-of-the-art pre-processing filters were tested and compared.

### 5.3 Tests & Results

A subset of the recorded sEMG data was used, and different filter types were tested in order to reduce noise in the raw recordings. Different types of Buttersworth filters were tested, as can be seen in figure 9 & 10.

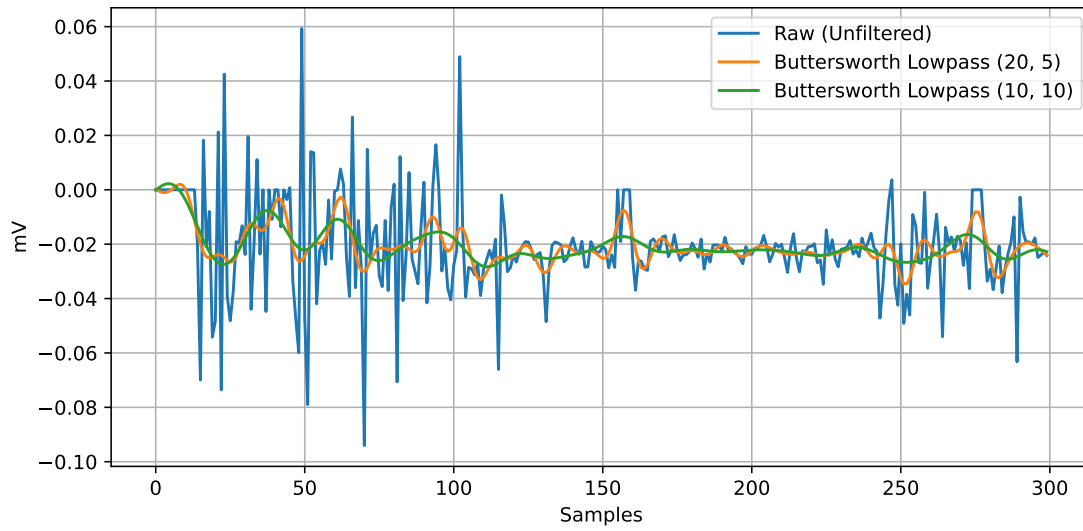


Figure 9: Comparison of Buttersworth low-pass filters of different cutoff frequencies and orders.

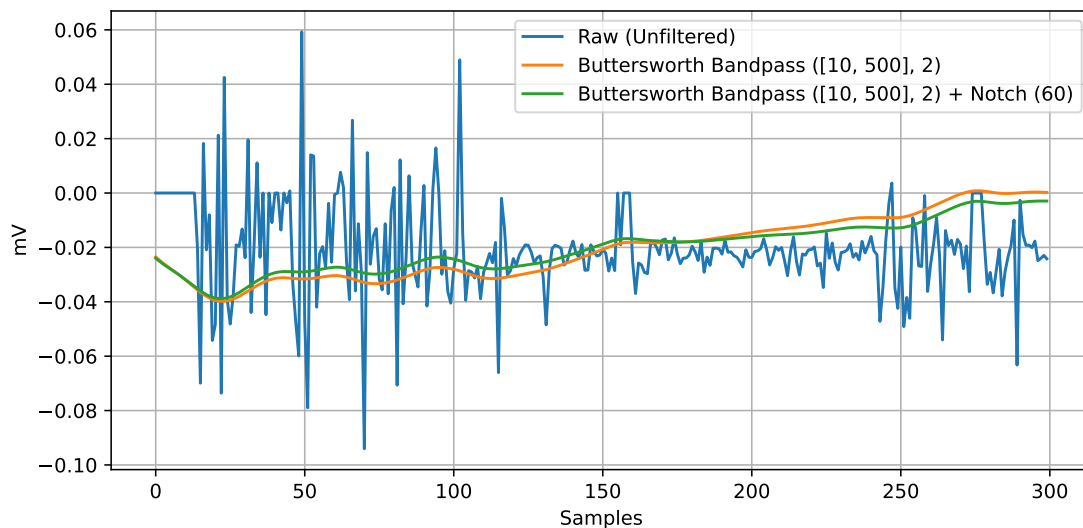


Figure 10: Comparison of Buttersworth band-pass filters of different cutoff frequencies, orders and the usage of a Notch filter.

## 5.4 Evaluation

As can be seen in the figure, different configurations of pre-processing filters have a large impact on the resulting filtered sequence. It can be seen in figure 9 that most of the change in amplitude exists in the low frequencies, and these are removed due to using a low-pass filter. Furthermore, it can be seen that the intent of the signal is kept when a filter order of 5 is used, compared to a filter order of 10. When comparing the two low-pass filters, it can be determined that using a cutoff frequency of  $20Hz$  and a order of 5 is a ideal for sEMG signals due to the amount of large frequencies in the recordings. Alternatively, Buttersworth band-pass filters are tested in figure 10,

## 5.5 Cleaning of Motive Capture Data

TODO: HERE I NEED TO GO ALL IN ON DATA CLEANING

## 5.6 Dataset used for Training

Due to the problems with the Motive motion capture software explained in section 4.4.2, it was determined that the main dataset for training the chosen methods would be based on dataset [30] from the paper [27]. The dataset contains sections of sEMG data and kinematic movements of the hand. These sections are labeled as either *reaching*, *manipulation* or *releasing*. Due to the dataset containing data for regression and classification, it is possible to explore multiple methods of HMI's. The pre-processing step is not covered for the training dataset [30], as the dataset has been pre-processed using a 4th-order band-pass filter with a band of 25 to  $500Hz$ , then the data was subject to a 4th-order low-pass filter at  $8Hz$ . The main objective of these tests are to review and compare possible methods of regression & Classification of sEMG data in order to determine the movements of the hand.

# 6 Machine-Learning Intent Classification

Due to the dataset containing labels associated with movements of the hand, it is possible to use the dataset to train a intent prediction classifier. As mentioned in the papers [17] & [15], it is ideal to feature extract windows of the raw sEMG data. The papers propose that the features *Zero Crossing* & *Root Mean Square* are ideal for intent classifiers. Furthermore, the paper [16] proposes that the Machine-Learning classifier LDA has the highest classification rate out of similar methods. The paper [17] proposes the use of the SVM ML method for intent classification. Both types of classification will be explored and compared.

TODO: Why these features?

## 6.1 Implementation

In order to classify intent from sEMG muscle data, the data needs to be converted to feature space before it can be used as input to a machine learning algorithm. For

this, it was chosen based on state-of-the-art literature, that the feature extraction methods would be zero-crossing & RMS. The input channel for a single sEMG window was converted into a vector of zeros and ones for the zero-crossing features, where a one is set if the data crosses over the zero line. Furthermore, the RMS for a window was calculated, and inserted to the end of the input vector. This effectively converts the 6 sEMG channels of a window size of  $N$  into a feature vector of size  $N + 1$ . The feature-based inputs were extracted, and their movement labels were used as the target classification. The resulting classification structure can be seen in Figure 11.

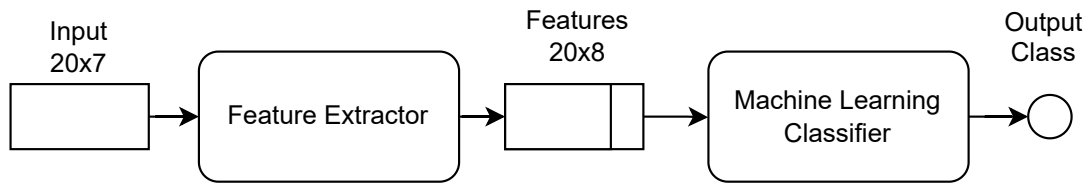


Figure 11: The machine learning classifier setup with a feature extraction step.

The dataset of features and ground truths were then used as input for discriminant analysis, and SVM classifiers. The purpose of **discriminant analysis** is to classify inputs into groups. Discriminant analysis is a classical multivariate method of Supervised Learning, that takes a input set with their ground-truth classes and tries to maximize separation between these different classes. The models assumes that data follows a Gaussian distribution. For this ML method, two types of discriminant analysis were tested on the dataset, namely LDA & quadratic discriminant analysis (QDA). The main difference between LDA and QDA is that LDA makes the assumption that the covariance matrices of the classes are the same. Equal covariance matrices will result in linear separations between classes. QDA as an alternative does not assume this equal covariance, this results in a classifier that assumes quadratic separations between classes. Just as discriminant analysis, SVM based methods are used to separate inputs into groups based on classes. SVM is a robust supervised learning method that groups dataset classes. SVM tries to maximize the width between classes by converting the input to a higher dimensional feature vector, and using this vector, the SVM algorithm is able to efficiently calculate a non-linear classification. The feature space conversion is determined by the choice of SVM kernel in the algorithm. For this ML method, 3 types of SVM classifiers were tested, a SVM using a Radial Basis Function (RBF) kernel, a SVM using a sigmoid Kernel and a NuSVM method with the RBF kernel and a parameter for the number of support vectors used.

## 6.2 Tests & Results

The methods are tested on 50 sets of data that was not part of the training set. The discriminant analysis methods can be seen in figure 12, with the average accuracy of the methods respectively being 61% & 55% over the 50 tests.

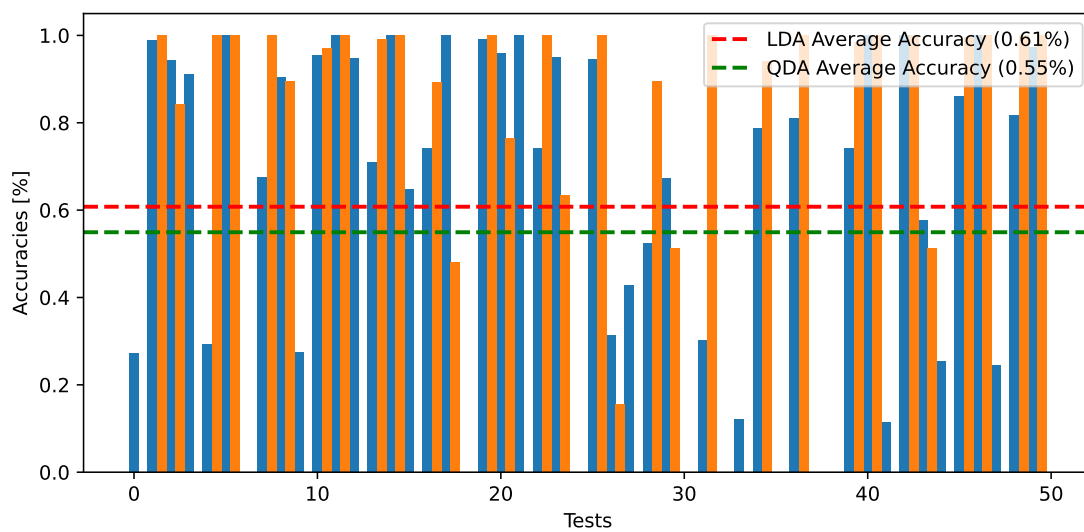


Figure 12: Comparison of discriminant analysis methods (QDA/QDA) over 50 tests.

The SVM methods can be seen in figure 13, with the average accuracy of the methods respectively being 54%, 56% & 59% over the 50 tests.

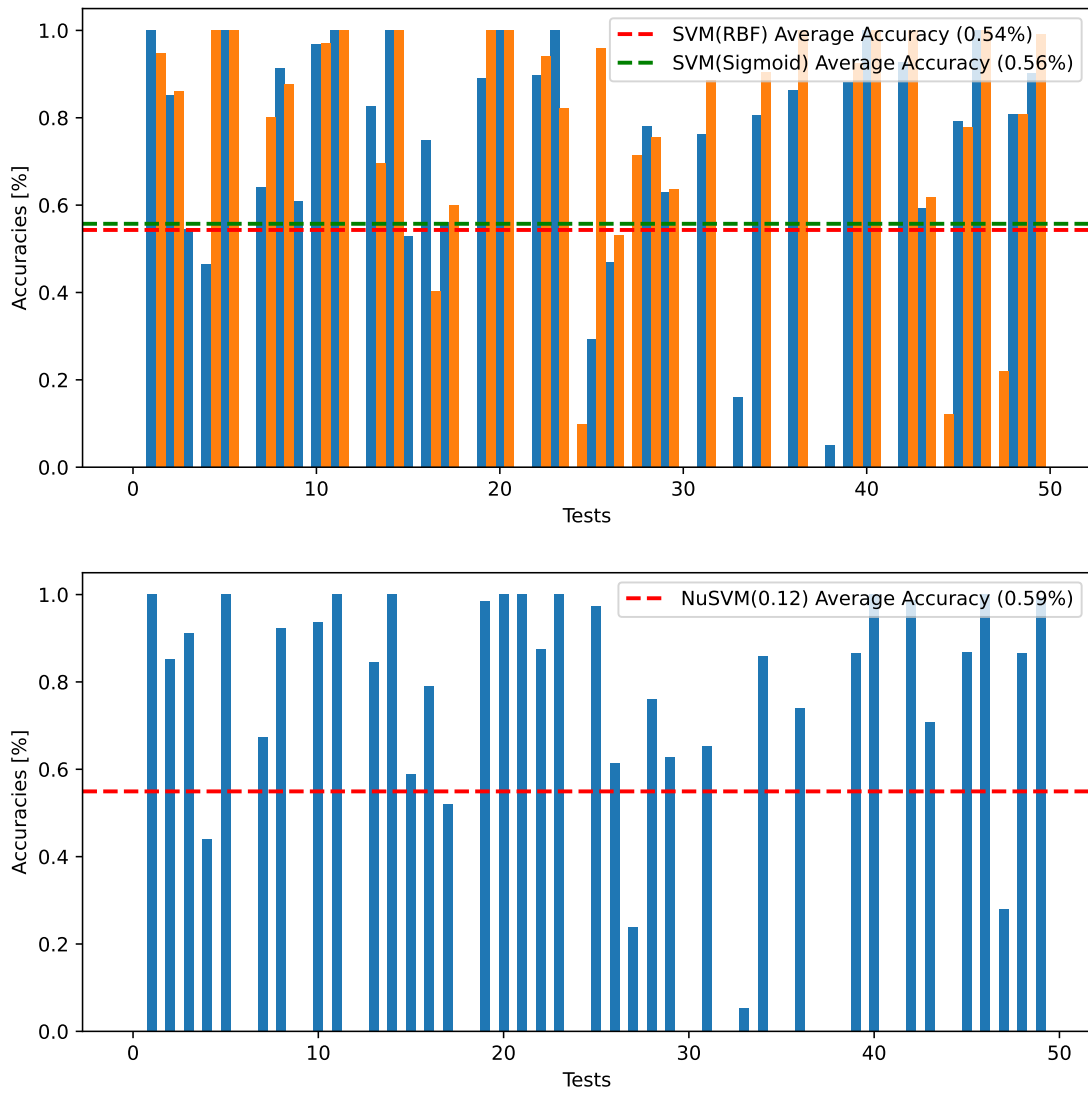


Figure 13: Comparison of SVM Kernels & parameters over 50 tests.

### 6.3 Evaluation

The methods tested can be seen to have similar average accuracy of  $\sim 60\%$  over 50 tests. Because of this, it is difficult to choose a superior method without further analysis. The choice of machine learning method depends on its overall classification rate over 50 tests, but it can also be important to rate the ML methods based on their inter-quantile values. A full comparison of the machine learning methods can be seen in figure 14.

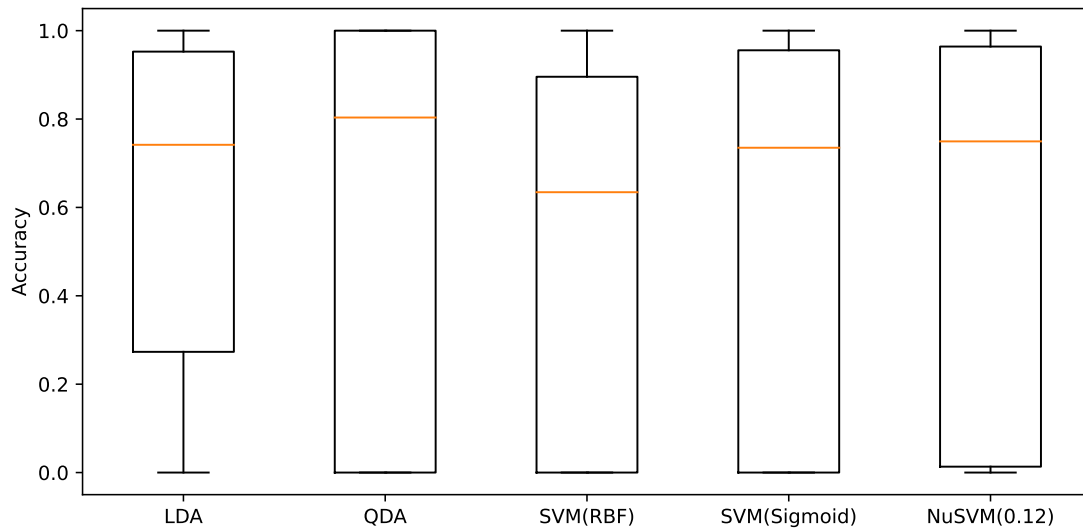


Figure 14: Comparison of chosen classification methods based on accuracy over 50 tests.

It can be seen in the boxplot that most methods have a similar inter-quantile median, and fairly small whiskers. In order to get a clearer comparison of methods, the relevant values have been compared in table 3.

ML Method	avg-accuracy [%]	Inter-quantile Median	Inter-quantile Range
LDA	<b>61%</b>	0.741705	<b>0.679410</b>
QDA	55%	<b>0.803432</b>	1.000000
SVM (RBF)	54%	0.634426	0.895688
SVM (Sigmoid)	56%	0.735050	0.955580
NuSVM (0.12)	59%	0.749436	0.950715

Table 3: Comparison of relevant classification parameters for the chosen methods. The best performing parameters have been highlighted.

The relevant parameters in the table makes it possible to identify the most suitable method for intent classification. It can be seen that LDA has the overall best accuracy of all the methods of 61%, and the overall worst performing method is SVM (RBF). By denoting the median and the range of the inter-quantile section of the boxplots, we can further elaborate on the accuracy of the 50 tests. LDA has the best average accuracy, and it also has the smallest inter-quantile range, indicating that LDA perform well across tests with a robustness to outlier tests. It can be seen that QDA performs best according to the inter-quantile median, but QDA is also the method that has the largest inter-quantile range indicating that QDA is not very robust to outlier tests. An alternative to the discriminant analysis methods, it can be seen that the NuSVM method with a number of support vectors denoted by 0.12. NuSVM has the second best average accuracy, the second best inter-quantile median & the third lowest inter-quantile range. From the table 3, it becomes apparent that

none of the methods have ideal performance, but that the LDA method is the best method for intent classification. This result is similar to the conclusion in paper [10]. The resulting performance metrics of the ML methods are dependent on the chosen feature extraction techniques used. Zero crossing and MSE features can be used for the classifiers and provide insight into what parameters are important when working with sEMG data.

## 7 Neural Network Movement Regression

### 7.1 Windowed Convolutional Neural Network

As an alternative to intent classification, the dataset could be used to train finger movement regression networks.

#### 7.1.1 Implementation

The sEMG data used as input for regression networks is complex. The sequences of muscle activity needs to be understood by the proposed method and produced into a an output. A network type that is ideal to understand complex meaning in, 3-dimensional inputs is a CNN network. A CNN consists of a set of Convolution Layers that deforms inputs to abstract convolution features. The structure is considered sparsely connected due to the convolution layers are only receiving a subset of the previous convolution features. The feature conversion is ideal when a network needs to become robust and needs to recognize larger concepts in the input. This functionality is especially used when the input data takes the shape of a matrix. Once the input is convoluted to a chosen feature abstraction, it is given to a MLP structure trained to convert the convolution features into a usable output. CNN networks have no build-in time-based functionality, they receive a set of inputs and produce an output. It is possible however to represent time if the input is given in segments consisting of multiple time-frames. Because of this, the sEMG muscle activity from the dataset is segmented into windows of a desired size, the output angles that the network should do regression towards are then chosen to be the first angle after the window. A CNN network can be used in the field of sEMG processing due to the convolution layer's ability to learn abstract formations of the sEMG data. The network would be able to identify patterns in sEMG data and correlate them to an appropriate output. The CNN network structure seen in figure 15.

TODO: Why did my network end up looking like this?



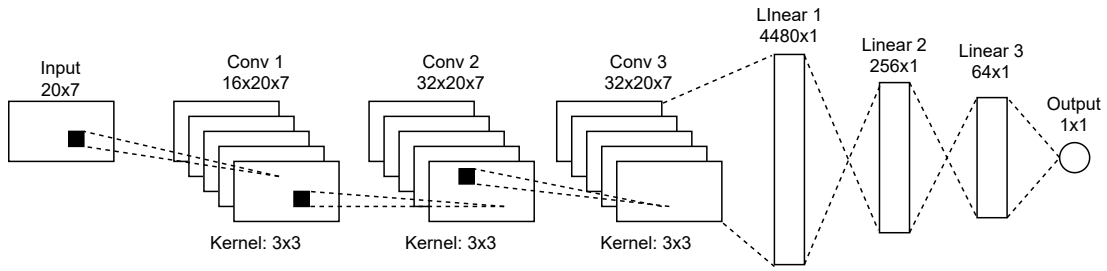


Figure 15: The chosen CNN network structure, consisting of 3 Convolution Layers and 3 Linear layers. Network input is a window of sEMG recordings, with the purpose of regression of a finger joint angle.

As visualized in the figure, the CNN network consists of 3 Convolution layers followed by 3 MLP layers. The chosen CNN network structure is chosen to be simple due to the small input window of 7 muscle sensors and a window size of 20 samples. For this reason, no pooling was used between the convolution layers. The Convolution layers extract features up to a size of 32 using a convolution kernel with a size of [3, 3]. The convolution features are then flattened, to a size of 4480, before being subject to the MLP layers that convert the extracted features into a regression prediction.

The CNN network is trained to do regression of joint angles of the hand, because of this, the loss function is determined to be MSE loss. The network is trained using an Adam optimizer with a learning rate of  $1e^{-4}$ . A subset of the dataset is split into a test and a validation set, and windows are extracted correlating input and output. The output is normalized, and the input/output sets are shuffled before training takes place.

### 7.1.2 Tests & Results

In order to test the CNN network and assess its performance, the training MSE loss can be seen in figure 16.

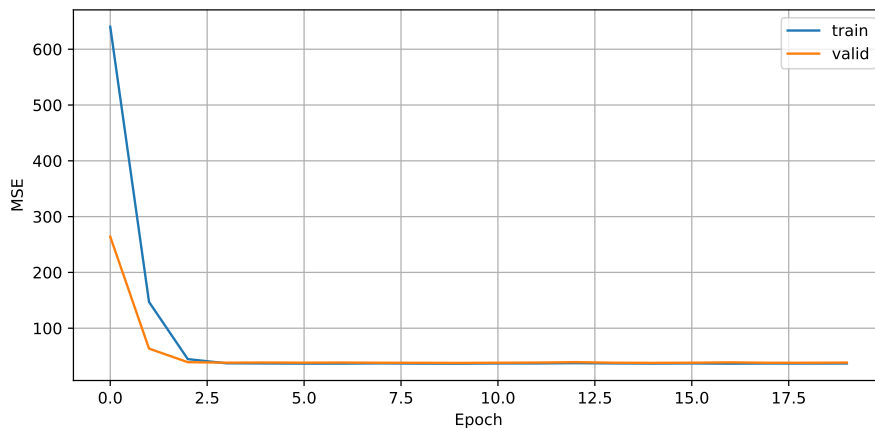


Figure 16: The Train and Validation MSE loss during training of the CNN network method.

TODO: Maybe remove this

The CNN network is trained with a batch size of 8 over 20 epochs, but as can be seen in the figure, the MSE loss settles at  $\sim 34$  after just 3 epochs.

50 sets of regressions that have not been trained on are taken from the dataset for testing. The errors of the dataset are plotted, as can be seen in figure 17.

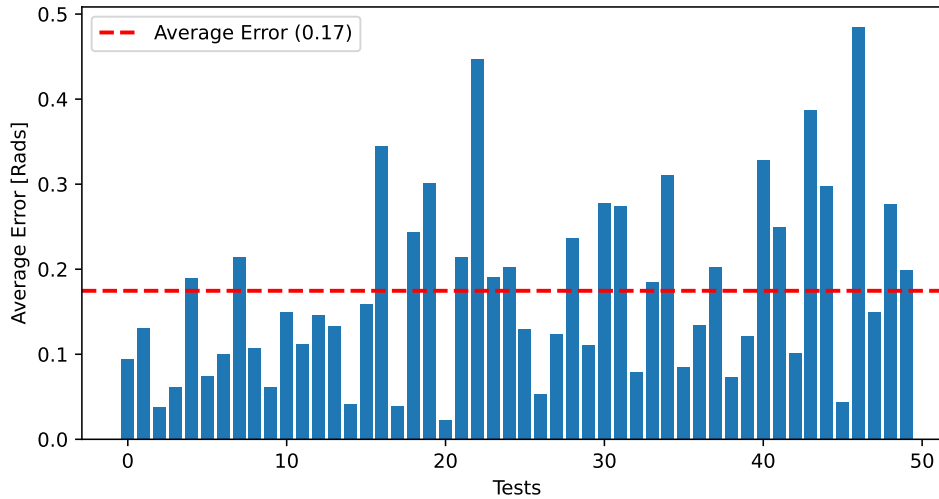


Figure 17: The errors of 50 regressions using the CNN network.

### 7.1.3 Evaluation

As can be seen in figure 16, the CNN network is able to be trained on the dataset with a validation set MSE loss of 34. The errors of the 50 test regressions in figure 17 show that a fairly large average regression error of 0.17 Radians exists in the test regressions, and that the average error is skewed upwards due to some outlier tests having large average errors up to 0.3 Radians.

## 7.2 Recurrent Neural Network Regression

Due to sEMG data being time-based, Recurrent network types are ideal for regression predictions. RNN networks are similar to MLP's with the main difference being that a RNN has hidden feedback memory state that is derived from earlier inputs. This functionality makes RNN networks ideal for concurrent, time-based systems where a sequential input distribution needs to be converted to a output regression. Another use case of RNN-based regression systems are systems where response time is critical. The RNN network does not use a window of data, it converts the input of the current time frame, and the feedback of the previous time frame into a prediction. Because of the hidden memory, a RNN network has a quicker response time than a window-based network. The RNN network structure designed to predict regression of finger movements from sEMG data can be seen in figure 18.

TODO: Why did my network end up looking like this?

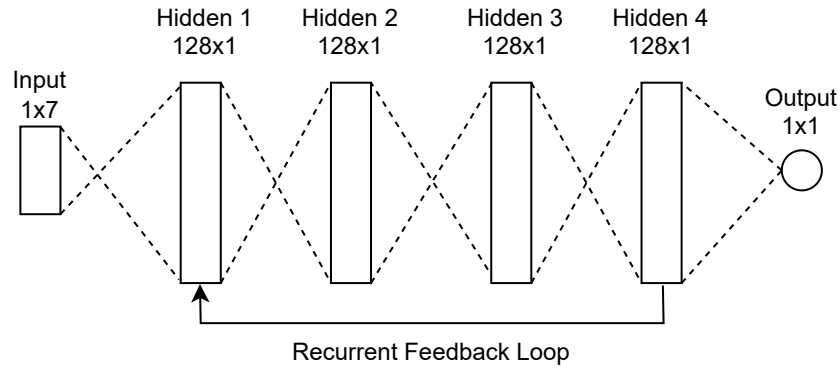


Figure 18: The chosen RNN network structure, consisting of a input layer, 4 hidden layers with a recurrent feedback loop, and a output layer.

### 7.2.1 Tests & Results

The RNN network is trained on the dataset [30], in a similar way as the CNN network, with the purpose of approximating finger angle regressions per time frame. The RNN network is trained with a batch size of 8, with the MSE loss function and the Adam optimizer with a learning rate of  $1e^{-2}$ . In order to test the network, a random set of 50 regressions that have not been trained on are taken from the dataset. The average errors of each regression test is plotted, as can be seen in figure 19.

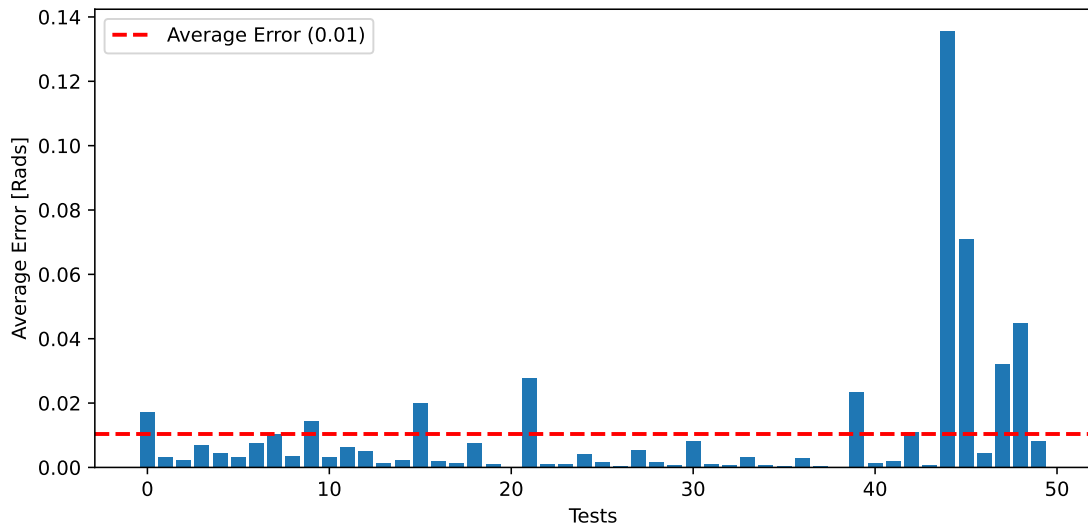


Figure 19: The errors of 50 regression tests using the RNN network.

### 7.3 Evaluation of Regression Methods

The errors of the 50 test regressions in with the different models can be seen in figure 20.

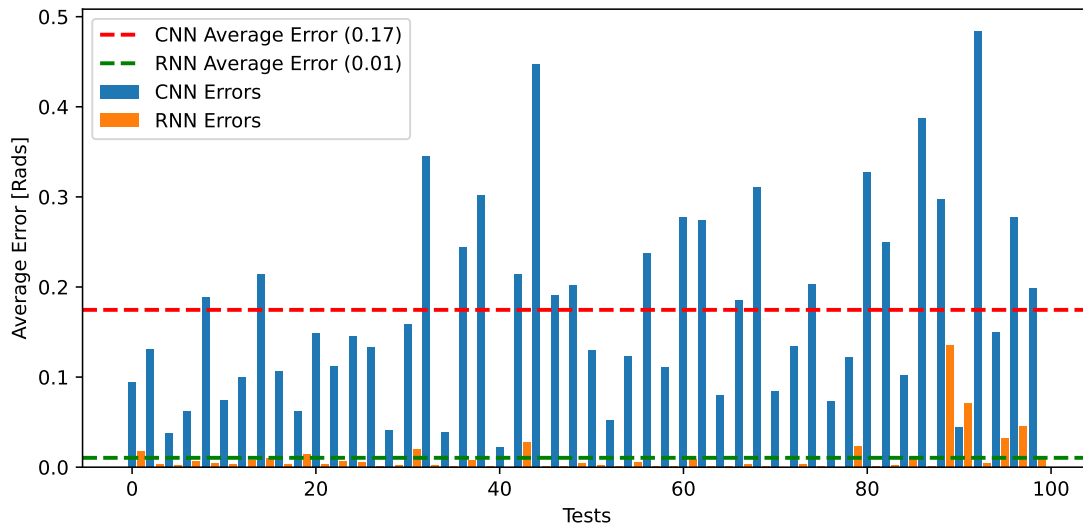


Figure 20: Comparison of Windowed CNN and RNN regression methods.

The figure clearly shows that there is a large difference in window-based and recurrent network types. The CNN shows a average test error of 0.17 Radians, while the RNN network has a average test error of 0.01 Radians. The reason for the large error in the CNN network test is unclear. One of the reasons the CNN network is unable to accurately learn regression could be because of the pre-processing done in the dataset. Alternatively, the network is unable to learn because of the window size. This would make sense since the RNN network with a really low error is able to learn to do regression, as it is not limited by a arbitrary window of input.

It becomes apparent that teaching a neural network to do regression of finger joints is a complicated task. Because of this, the tests propose that it is ideal to use a type of Recurrent Network for regression.

## 8 Simulated Prosthetic Hand

### 8.1 Useability of the Simulated Prosthetic Hand

Access to existing prosthetic hand simulations proved to be impossible to access and use, as explained in section ??, they are either unavailable because their associated products have been discontinued or locked behind a pay-to-access barrier where you have to pay to receive a real prosthetic. Due to non-availability of prosthetic hand simulations, it was chosen that through this thesis, a open source prosthetic hand needed to be created for testing of the algorithms developed as part of this project. The creation of a prosthetic hand simulation can be seen in section 4.6. The prosthetic hand was designed to be as anatomically similar as a real hand as possible. This was done in order to accurately simulate the movement of a real hand, and because of it, allow users to test and validate control methods on a simulation before needing to construct a real prosthetic. The usability and dynamic movement of the simulated prosthetic hand needs to be assessed. This is important because the usability of a prosthetic hand has a large impact on rehabilitation for the end-user.

### 8.2 Method

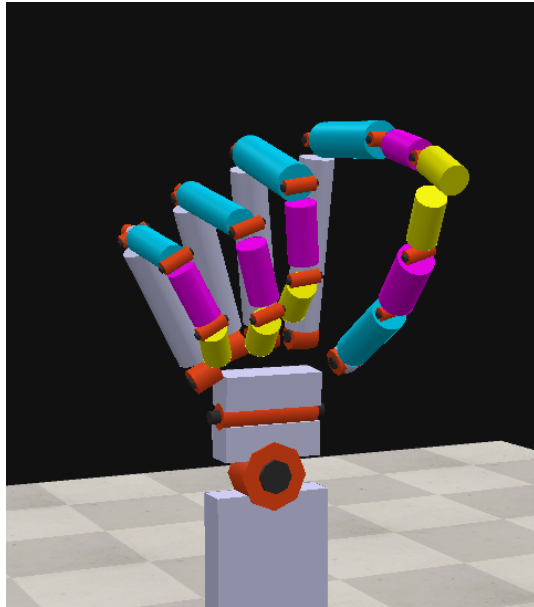
In order to test the usability and dynamic movement of the simulated prosthetic hand, the hand was tasked with achieving the end-poses of the most used day-to-day grips. These grips were explained in section 4.4 table 2, namely the *Pulp pinch*, *Lateral pinch*, *Five-Finger pinch* & *Diagonal Volar grip (Power grip)*. In order to pose the simulated hand, the interface created in ROS2 was used to send kinematic configurations to the hand simulation.

### 8.3 Test & Results

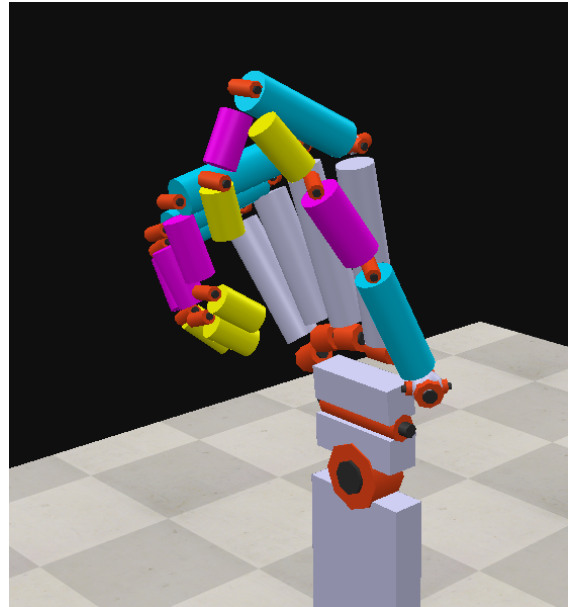
The hand was posed into all 4 day-to-day grip configurations for visual assessment. The resulting configurations of the hand can be seen in figure 21. The software used to pose the hand simulation can be seen in appendix C

### 8.4 Evaluation

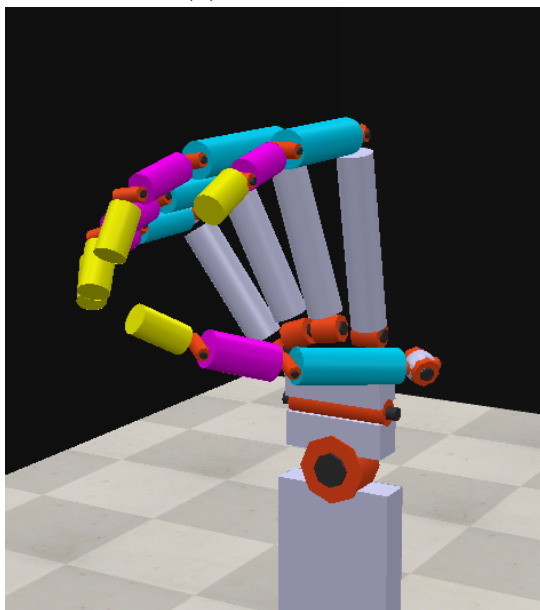
Based on a visual assessment of figure 21, it can be concluded that the prosthetic hand is able to be posed similarly to the real-life reference. The ROS2 interface created for the simulation allows for easy manipulation of the joint rotations, and because of this, achieving different poses becomes easy to do. The hand simulation is able to achieve a wide range of motion because of its design and its ability to mimic the anatomy of the real hand. From this it can be concluded that the prosthetic hand is proportionally correct and thus also allows for accurate posing, applicable in different day-to-day scenarios.



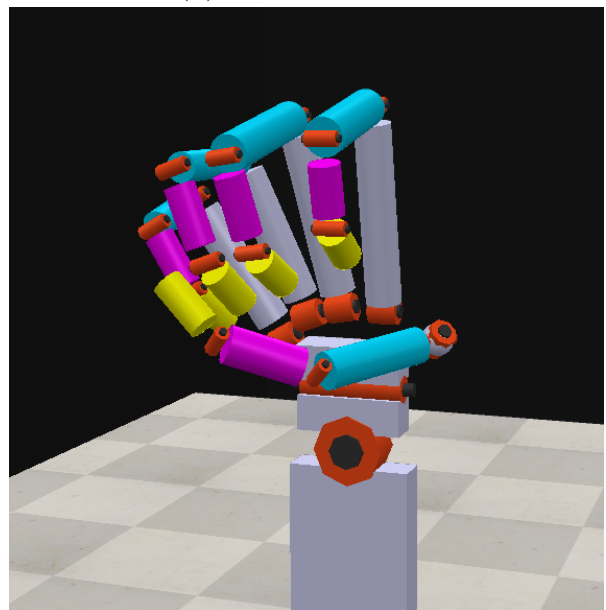
(a) Pulp pinch



(b) Lateral pinch



(c) Five-Finger pinch



(d) Diagonal Volar grip (Power grip)

Figure 21: The four most used day-to-day poses, tested in a hand prosthetic simulation.

## 8.5 Posing based on Network Output

TODO: More here..

As a result of testing different network types and their applicability for creating suitable motor control output for a prosthetic hand, it would be ideal to test the network output on the prosthetic simulation. For full video see appendix ??.

## 9 Discussion

The main purpose of this thesis is to research and experiment with state-of-the-art sEMG-based human-machine-interfaces for development of prosthetic devices. The experimentation is mainly done with the focus of identifying and modeling the intent & movement of the fingers. During the development of this thesis, several problems occurred with the choice of simulation tools. The initial chosen simulation software was the Gazebo [21] due to its close integration with ROS2 [20], and its use in modern robotics simulation tasks. After a lot of long-term problems and complications caused by the chosen software, a decision to switch to CoppeliaSim [22] was made. The change to CoppeliaSim solved a lot of the problems caused by Gazebo, the setup of the simulation and development of the kinematics became much clearer. Furthermore, setting up the controller of the prosthetic could be done using the build-in ROS2 communication.

Another problem had a large impact on the development of this thesis. In order to capture the movements of the fingers for the dataset, the product Motive Motion Capture Setup [28] was chosen, due to recommendation, availability and its use in state-of-the-art industry motion capture. The Motive setup consists of a camera rig designed to locate 3D markers in the scene. As a recording target, a glove was fitted with 3D markers. This was done in order to record the kinematic movements of the hand, a glove is fitted with 3D markers at the joints of the fingers. The main problem is that the setup is designed to capture large objects such as full-body tracking suits and larger static objects. Because of this, the 3D optimization algorithms used by the cameras has a tendency to remove markers that are close. This would cause the 3D markers of adjacent fingers to be combined into a single marker. The only way to solve this is to reduce the amount of markers on the glove.

In addition to not being able to have multiple fingers in the recording, the 3D marker labeling proved to be unreliable. The markers are shifting in labels if they disappear for a few frames at a time. This problem scaled with the length of the recording session, a 15 second recording of 7 markers would be recorded as 100+ labels in the resulting tracker output. In addition to the tracking being unreliable, the Motive software is unable to provide an effective label correction tool. Label rendering & correction tools is developed as part of this thesis, and is used to clean up a subset of the recorded dataset. Due to the extensive work needed to record and clean the movements of the hand, it became impossible to create a dataset large enough to train models on, and to create a general purpose dataset with recordings from multiple people. The time-consuming process of creating a simulated prosthetic and recording a dataset resulted in some of the goals of this thesis as explained in section 2.2 to not be fulfilled. It was not possible to fully test the simulated prosthetic device with real-time predictions from a model. Furthermore, it was not possible to fully test different pre-processing methods and their differences when used for training a model.

### Classification Tests

Multiple different machine learning methods is tested in section 6 The data is converted to a feature space set consisting of ZC and mean square error (MSE), and



is then used as input to a machine learning algorithm to create a lower-arm intent classifier. The accuracy of the resulting classifiers could have been improved, if more types of feature extractions had been tested. Furthermore, different types of machine learning classifiers and network based classifiers could have been tested in order to improve classification accuracy.

### **Regression Tests**

Different regression network models were trained to do regression of finger joint angles. These tests can be seen in section 7. Window based regression network methods were compared to recurrent network based methods. The window based regression has a large error, and it is unclear what the exact cause is. The large error could be result of using an incorrect size of window, or the result of the training data not being optimal for training. The error could also be the result of the training parameters used, and it might have been solved by extensive parameter tuning. The use of a recurrent network proved to have very accurate results for regression of finger angles.

### **Hand Simulation Tests**

The simulated hand created in CoppeliaSim [22] is tested in section 8. The hand is designed to be anatomically proportional to a real hand, with the same amount of degree of freedom as its real counterpart. The tests were created to assess the simulated prosthetic hand's ability to be manipulated and its ability to perform anatomically correct poses. The hand was manipulated to the 4 most used day-to-day grip types with great precision by a visual assessment. The main problem with the hand simulation is that it was not possible to test its performance using the output of a regression model as a controller. This was not possible due to the created dataset.

## 10 Conclusion

This thesis is developed with the purpose of researching & designing a state-of-the-art sEMG-based HMI for a simulated prosthetic hand. During the development of this thesis, a controllable prosthetic hand was developed in the simulation tool CoppeliaSim [22], that is able to be controlled by the commonly used robotics communication software ROS2 [20]. The prosthetic hand is designed to have anatomically correct proportions, with anatomically correct joints that allows the simulation to act and be controlled with similar movements as a real hand. The simulation is created with the purpose of providing an easy-to-use, freely available, advanced prosthesis simulation for others to use, modify and develop with. Another purpose of this thesis is to research and test state-of-the-art HMI techniques in the field of AI and ML, in order to compare and test different methods of converting sEMG based muscle activity into a usable controller scheme for a prosthetic device. This thesis tests two different areas of HMI interfaces, ML based lower-arm intent classification and AI based finger movement regression. Different models in each area are tested and compared, based on recommendations of state-of-the-art literature, in order to determine what models are ideal for the control of a prosthetic hand.

Several different ML models were trained and compared in section 6. All models were trained on feature-space converted sEMG data. Based on the tests and comparison of the classification accuracy table 3, it can be seen that the Linear Discriminant Analysis (LDA) performs best with an accuracy of 61% and inter-quantile range of 0.679. It can also be seen, and that QDA performs best in the inter-quantile median with a value of 0.803, but has the largest inter-quantile range. From this, the LDA machine learning algorithm is proposed to be best at intent classification of the lower-arm. As an alternative to intent classification, different AI models designed to do regression of finger movements were trained and compared in section 7. Based on the regression comparison in figure 20, it can be seen that Recurrent methods perform best compared to window based methods. This can be seen when comparing the average error in 50 tests, the CNN network has an average error of 0.17 Radians per test, where the RNN network has a low average error of 0.01 Radians.

The designed models are trained and tested using a freely available dataset [30]. This was done due to problems with the chosen Motive Motion Capture setup, these problems were reduced by the implementation of a rendering and cleaning software explained in section 5.5. Using this implemented software, it is possible to fix wrong labels and removing labels all together, compared to the building functionality in Motive. With this implemented software, it was possible to clean a small subset of recorded data, but it was not possible to create a full dataset of multiple people.

TODO: Emphasis on what the result of my thesis is! What specifically am i proposing to use in further research?

## 10.1 Future Work

Due to the problems encountered with the chosen software in this thesis, some parts of the motivation goals in section 2.2 were not possible to explore. Had it been easier to create a custom dataset, preferably with recordings from multiple people, it would have been possible to explore further combination of the created prosthetic and the trained models.

Further testing, of the dynamic control of a trained model in a simulated environment could also have been explored. This could be done in real-time, where a trained model could be used to convert live sEMG recordings into movements for the simulated prosthetic, allowing the test person to manipulate the simulated environment in real time. The work done in this thesis mainly explores two different areas of prosthetic controllers, classification based and regression based. Had a large dataset created specifically for the purpose of this thesis been created, it would be ideal to test the applicability of combining methods and by doing so, explore possible controller schemes that combines the individual movement of regression models and the robustness of intent classification.

TODO: More here!

# 11 Bibliography

## List of Figures

1	Example of a commercial prosthetic hand's manual control scheme [5].	8
2	The Ideal design of a prosthetic hand, that mimics the control scheme of a real hand. . . . .	9
3	A rendering of the anatomical joint structure of the hand. 2 DoF joints are colored in green, 1 DoF joints are colored in red, and passive 1 DoF joints are colored in blue. . . . .	17
4	Muscle diagram, containing the target sEMG locations. The numbering corresponds to the muscle names in Table 1. The left image shows the muscles on the rear of the arm, while the right shows the muscles on the front of the arm. . . . .	18
5	(a) Design and ideal 3D marker placements on the glove in order to calculate all the joint angles of the hand. (b) The created 3D marker glove with the chosen 3D marker locations. See section 4.4.2 for detail.	19
6	Visualization of the joint angle retrieval process. (a) the minimum bend of the Interphalangeal joint, (b) the maximum bend. The joint angle can be calculated from the 3D markers by denoting vectors from the center marker to upper and lower markers, and using Equation (1).	20
7	Created & anatomical reference design for the created simulated prosthetic hand. . . . .	23
8	Capture glove and sEMG sensors placed on the recording target. The sEMG sensors are located based on the muscles from table 1. . . . .	24
9	Comparison of Buttersworth low-pass filters of different cutoff frequencies and orders. . . . .	25
10	Comparison of Buttersworth band-pass filters of different cutoff frequencies, orders and the usage of a Notch filter. . . . .	25
11	The machine learning classifier setup with a feature extraction step. .	27
12	Comparison of discriminant analysis methods (QDA/QDA) over 50 tests. . . . .	28
13	Comparison of SVM Kernels & parameters over 50 tests. . . . .	29
14	Comparison of chosen classification methods based on accuracy over 50 tests. . . . .	30
15	The chosen CNN network structure, consisting of 3 Convolution Layers and 3 Linear layers. Network input is a window of sEMG recordings, with the purpose of regression of a finger joint angle. . . . .	32
16	The Train and Validation MSE loss during training of the CNN network method. . . . .	32
17	The errors of 50 regressions using the CNN network. . . . .	33
18	The chosen RNN network structure, consisting of a input layer, 4 hidden layers with a recurrent feedback loop, and a output layer. . . .	34
19	The errors of 50 regression tests using the RNN network. . . . .	34
20	Comparison of Windowed CNN and RNN regression methods. . . . .	35

21	The four most used day-to-day poses, tested in a hand prosthetic simulation. . . . .	37
----	--	----

## List of Tables

1	The muscles targeted with the 6 available sEMG sensors, as recommended by the papers [27] & [17]. The targeted muscles contributes to a lot of the movements of hand & lower-arm, and are ideal for the dataset. . . . .	18
2	The most used hand grips in day-to-day tasks based on <i>Southampton Hand Assessment Procedure</i> [11] & <i>Sollerman Hand Function Test</i> [29].	21
3	Comparison of relevant classification parameters for the chosen methods. The best performing parameters have been highlighted. . . . .	30

## References

- [1] *Grasping the Importance of Our Hands - Douglas G. Smith*. <https://orthop.washington.edu/sites/default/files/files/16-6-document.pdf>. Accessed: 2023-02-05.
- [2] Mr Kevin J Zuo and Jaret L Olson. “The evolution of functional hand replacement: From iron prostheses to hand transplantation”. In: *Plastic Surgery* 22.1 (2014), pp. 44–51. DOI: 10.1177/229255031402200111. eprint: <https://doi.org/10.1177/229255031402200111>. URL: <https://doi.org/10.1177/229255031402200111>.
- [3] *Prosthetic Leg Fit: Types of Knee Prosthesis for Leg Amputations - Alanna Holz*. [https://propelphysiotherapy.com/amputation/prosthetic-legs-types-of-knee-prosthesis/#\\_Mehcanical\\_Knees](https://propelphysiotherapy.com/amputation/prosthetic-legs-types-of-knee-prosthesis/#_Mehcanical_Knees). Accessed: 2023-05-20.
- [4] Cody McDonald et al. “Global prevalence of traumatic non-fatal limb amputation”. In: *Prosthetics and Orthotics International* Publish Ahead of Print (Dec. 2020), p. 030936462097225. DOI: 10.1177/0309364620972258.
- [5] *Ottobock bebionic Hand EQD*. <https://www.ottobock.com/en-us/product/8E70>. Accessed: 2023-05-20.
- [6] *Ottobock Hand prices*. <https://bionicsforeveryone.com/bionic-hand-price-list/>. Accessed: 2023-05-20.
- [7] *Rehabilitation - World Health Organization*. <https://www.who.int/news-room/fact-sheets/detail/rehabilitation>. Accessed: 2023-02-05.
- [8] Kristin Østlie et al. “Prosthesis rejection in acquired major upper-limb amputees: a population-based survey”. In: *Disability and Rehabilitation: Assistive Technology* 7.4 (2012). PMID: 22112174, pp. 294–303. DOI: 10.3109/17483107.2011.635405. eprint: <https://doi.org/10.3109/17483107.2011.635405>. URL: <https://doi.org/10.3109/17483107.2011.635405>.

- [9] M. Tech. "A Review paper on EMG Signal and its Classification Techniques". In: 2015.
- [10] Keun-Tae Kim et al. "Upper-Limb Electromyogram Classification of Reaching-to-Grasping Tasks Based on Convolutional Neural Networks for Control of a Prosthetic Hand". In: *Frontiers in Neuroscience* 15 (2021). ISSN: 1662-453X. DOI: 10.3389/fnins.2021.733359. URL: <https://www.frontiersin.org/articles/10.3389/fnins.2021.733359>.
- [11] *Southampton Hand Assessment Procedure (SHAP)*. <http://www.shap.ecs.soton.ac.uk/>. Accessed: 2023-04-14.
- [12] Zhaolong Gao et al. "A Multi-DoF Prosthetic Hand Finger Joint Controller for Wearable sEMG Sensors by Nonlinear Autoregressive Exogenous Model". In: *Sensors* 21.8 (2021). ISSN: 1424-8220. DOI: 10.3390/s21082576. URL: <https://www.mdpi.com/1424-8220/21/8/2576>.
- [13] *Thalmic Labs Myo gesture control armband*. <https://www.zdnet.com/article/thalmic-labs-shuts-down-myo-gesture-control-armband-project/>. Accessed: 2023-04-14.
- [14] *Delsys Trigno sEMG Recording System*. <https://delsys.com/trigno/>. Accessed: 2023-05-05.
- [15] Yuki Kuroda et al. "Coevolution of Myoelectric Hand Control under the Tactile Interaction among Fingers and Objects". In: *Cyborg and Bionic Systems 2022* (2022). DOI: 10.34133/2022/9861875. eprint: <https://spj.science.org/doi/pdf/10.34133/2022/9861875>. URL: <https://spj.science.org/doi/abs/10.34133/2022/9861875>.
- [16] Yanchao Wang et al. "Design of an Effective Prosthetic Hand System for Adaptive Grasping with the Control of Myoelectric Pattern Recognition Approach". In: *Micromachines* 13.2 (2022). ISSN: 2072-666X. DOI: 10.3390/mi13020219. URL: <https://www.mdpi.com/2072-666X/13/2/219>.
- [17] Iason Batzianoulis et al. "Decoding the grasping intention from electromyography during reaching motions". In: *Journal of NeuroEngineering and Rehabilitation* 15 (2018).
- [18] Zhen Ma et al. "Decoding of Individual Finger Movement on One Hand Using Ultra high-density EEG". In: *2022 16th ICME International Conference on Complex Medical Engineering (CME)*. 2022, pp. 332–335. DOI: 10.1109/CME55444.2022.10063299.
- [19] Maged S. AL-Quraishi et al. "EEG-Based Control for Upper and Lower Limb Exoskeletons and Prostheses: A Systematic Review". In: *Sensors* 18.10 (2018). ISSN: 1424-8220. DOI: 10.3390/s18103342. URL: <https://www.mdpi.com/1424-8220/18/10/3342>.
- [20] *ROS - Robot Operating System*. <https://ros.org/>. Accessed: 2023-04-14.
- [21] *Gazebo - Gazeboism*. <https://staging.gazebosim.org/home>. Accessed: 2023-04-28.
- [22] *Coppeliarobotics*. <https://www.coppeliarobotics.com/>. Accessed: 2023-03-21.

- [23] *EMGworks - Delsys*. <https://delsys.com/emgworks/>. Accessed: 2023-03-21.
- [24] *MediaPipe landmark tracking - MediaPipe Python*. <https://mediapipe.dev/>. Accessed: 2023-04-28.
- [25] *Motive:Tracker - OptiTrack*. <https://optitrack.com/>. Accessed: 2023-03-21.
- [26] *Forearm Muscles - Anatomy and Function*. <https://boneandspine.com/forearm-muscles/>. Accessed: 2023-05-20.
- [27] Nestor Jarque-Bou et al. “A calibrated database of kinematics and EMG of the forearm and hand during activities of daily living”. In: *Scientific Data* 6 (Nov. 2019). DOI: 10.1038/s41597-019-0285-1.
- [28] *Motive Tracker Software - OptiTrack*. <https://optitrack.com/software/motive/>. Accessed: 2023-03-21.
- [29] *Sollerman Hand Function Test*. [https://www.physio-pedia.com/Sollerman\\_Hand\\_Function\\_Test](https://www.physio-pedia.com/Sollerman_Hand_Function_Test). Accessed: 2023-04-25.
- [30] Nestor Jarque-Bou et al. *A calibrated database of kinematics and EMG of the forearm and hand during activities of daily living*. Version 1.0. Zenodo, July 2019. DOI: 10.5281/zenodo.3337890. URL: <https://doi.org/10.5281/zenodo.3337890>.
- [31] Ashirbad Pradhan, Jiayuan He, and Ning Jiang. “Multi-day dataset of forearm and wrist electromyogram for hand gesture recognition and biometrics”. In: *Scientific Data* 9 (Nov. 2022), p. 733. DOI: 10.1038/s41597-022-01836-y.
- [32] Zhaolong Gao et al. “A Multi-DoF Prosthetic Hand Finger Joint Controller for Wearable sEMG Sensors by Nonlinear Autoregressive Exogenous Model”. In: *Sensors* 21.8 (2021). ISSN: 1424-8220. DOI: 10.3390/s21082576. URL: <https://www.mdpi.com/1424-8220/21/8/2576>.
- [33] Iason Batzianoulis et al. “Decoding the grasping intention from electromyography during reaching motions”. In: *Journal of neuroengineering and rehabilitation* 15.1 (2018), pp. 1–13.

# Appendices

The appendices should have been supplied with the report. Alternatively, see <https://github.com/thom9258/masters-thesis/tree/main/report/appendix> for online reference.

- A Prosthetic Hand Simulation in CoppeliaSim**
- B Hand Simulation Poses**
- C ROS2 Controller for the Prosthetic Hand**
- D Modification & Replaying Scripts for Motive CSV Files**
- E Motion-Capture & sEMG Dataset**
- F Motive Marker labeling & Uncleaned marker set**
- G Pre-Processing Filter Graphs**
- H Network Creation/Training/Testing Code**